2020

Development of a Torque-Based Device for the Quantification of Arm Rigidity in Patients with Parkinson's Disease

Georgina O. Miller
Virginia Commonwealth University

Development of a Torque-Based Device for the Quantification of Arm Rigidity in Patients with Parkinson's Disease

A thesis submitted in partial fulfillment of the requirements for the degree of Master of Science at Virginia Commonwealth University

By

Georgina O. Miller
Bachelor of Science, General Engineering, Sweet Briar College, 2011

Director: Paul A. Wetzel, Ph.D.
Associate Professor, Department of Biomedical Engineering

Virginia Commonwealth University
Richmond, VA
May 2020

Acknowledgements

I would like to express my deep gratitude to Dr. Paul Wetzel for his continuous support and guidance throughout my research. His vast knowledge especially that of systems engineering, electrical engineering, neurodegenerative brain disorders, and human factors has taught me more than I thought possible. He has also been a mentor to me throughout my graduate career at VCU and I know without his guidance I would not have made it to this point.

In addition to my advisor, I would like to thank my thesis committee: Dr. Mark Baron and Dr. Ding-Yu Fei for their support.

To my fellow classmates and lab mates, especially George Weistroffer, thank you for all the thought-provoking conversations, collaborations, assistance, and words of encouragement.

I would also like to express my sincere thanks to ADVANCED Motion Controls®, for supplying the controller through their university outreach program that allowed us to continue the device build and complete this research project.

Lastly, I would like to thank my family and friends, especially my parents and Alex. To my parents, thank you for all the love, support, and advice that you have shown me not only during my graduate studies but throughout my entire life. Your continued support above and beyond that of even the most wonderful parents is truly the only reason I am where I am today. Without you, I would not have learned the values of hard work and determination and without your support during my failures I would not know the true value of success. To Alex, thank you for sticking by my side through the many long years of my academic life. I know the past six years of distance has not been easy but your support throughout this process has meant the world to me and I appreciate it more than words can express.

Table of Contents

List of Figures

List of Tables

Abstract

Development of a Torque-Based Device for the Quantification of Arm Rigidity in Patients with Parkinson's Disease

Georgina O. Miller, M.S.

A thesis submitted in partial fulfillment of the requirements for the degree of Master of Science in Biomedical Engineering at Virginia Commonwealth University

Major Director: Paul A. Wetzel, Ph.D., Associate Professor, Department of Biomedical Engineering

Virginia Commonwealth University
Richmond, VA
May 2020

Parkinsonian rigidity is caused by the inability of the muscles to relax and extend properly, due to reduced dopamine levels and often begins on one side of the body before spreading contralaterally. The current standard for determining joint rigidity in a clinical setting is a test completed by the clinician based on the feel of the relaxed wrist and elbow joints as they are passively flexed and extended and a series of ordinal rating scales, the Movement Disorder Society's – Unified Parkinson's Disease Rating Scale (MDS-UPDRS), Hoehn and Yahr Scale (H&Y), and Parkinson's Disease Questionnaire-39 (PDQ-39). These methods are used to determine the severity of the patient's disease and the impact it has on their quality of life, but they lack objectivity and do not differentiate between individual symptoms. We present a torque-based device to objectively quantify rigidity in a PD patient's arm. The device employs a servo motor-shaft assembly, connected to a rigid forearm sling, and controlled by a computer to passively flex and extend the elbow joint laterally. Two individuals were used for preliminary results in lieu of the patient restrictions due to COVID-19. A sine, ramp, and random (sine-like) stimuli were used on each person during a relaxed phase, and a co-contracted or clenched-fist phase. A torque transducer and potentiometer measured the torque and position with respect to time while angle of rotation, acceleration,

and velocity of the shaft were monitored simultaneously to ensure safety. Results showed that the magnitude of rigidity was greater during co-contraction than during relaxation indicating that rigidity can be objectively measured using this device. Quantifying joint rigidity will allow for a better understanding of the mechanisms of rigidity in Parkinson's and other movement disorders.

I. Introduction

Parkinson's Disease (PD) is a neurodegenerative condition, with no cure, brought on by the selective death of dopaminergic neurons in the substantia nigra region of the midbrain. PD occurs most often in those over the age of 50, with the average age of onset at 60, and affects more than 10 million individuals worldwide and more than one million individuals in the United States making it the second most prevalent neurodegenerative disease in the U.S. behind Alzheimer's Disease (Elkouzi, n.d.). In addition to a few environmental factors, some genetic factors have been identified, though they are extremely rare occurring in only 5-10% of patients (Tysnes & Storstein, 2017). The presence of Lewy bodies made up of clumping alpha-synuclein proteins in the substantia nigra is also considered a possible link to PD but the significance of these Lewy bodies and their increased presence in the substantia nigra is not well understood (Tysnes & Storstein, 2017).

Symptoms of Parkinson's Disease

Despite a lack of understanding concerning the cause of PD itself, significant research has been conducted to determine the cause of PDs hallmark symptoms. The dopaminergic neurons in the substantia nigra are responsible for secreting dopamine, a neurotransmitter vital to many pathways in the brain including those involved in motor control, motivation, and reward (Perry, 2015). During motor control, nigral neurons use dopamine to interact with movement regulating neurons in the basal ganglia as part of the biochemical sequence that allows for fine motor control (Triarhou, 2000-2013). Without this communication between the substantia nigra and basal ganglia, movements would be delayed and uncoordinated (Perry, 2015). As a result of the substantial decrease in dopamine levels, caused by

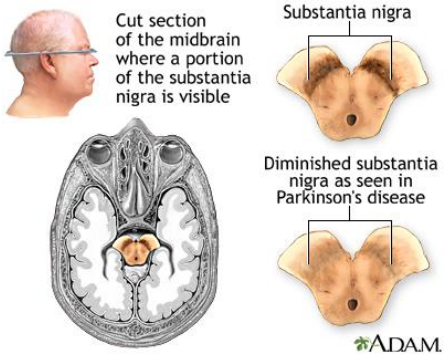

Figure 1: Decreased dopaminergic neurons cause a lack of pigmentation in the brain (https://medlineplus.gov/ency/imagepages/19515.htm)

dopaminergic neuronal cell death, a decrease in this essential biochemical communication occurs leading to the presence of the corresponding symptoms.

PD symptoms are divided into two main categories, motor symptoms including, bradykinesia, tremor, rigidity, dystonia, dyskinesia, freezing, masked face, shuffling gait, postural instability, and soft speech; and non-motor symptoms including, constipation, excessive sweating, fatigue, hallucinations and delusions, mood disorders such as depression and anxiety, sleep disorders, and vision problems all of which can worsen as time progresses (Spears, (n.d.) a ; Spears, (n.d.) b). As the disease state progresses and the presenting symptoms worsen, the increased disability and complications that arise often deteriorate the patient's quality of life (QoL) (Bhidayasiri & Martinez-Martin, 2017).

Symptom Presentation

Parkinson's Disease is known as an individual condition, meaning symptom presentation varies from one patient to the next and presented symptoms appear and evolve at different rates for each patient as well, although most individuals don't begin noticing symptoms until years after they develop PD (Barmore, n.d.). There is evidence that the initiation of dopaminergic neurodegeneration occurs decades before the manifestation of any motor symptoms, presenting non-motor prodromal symptoms that alone would not necessarily point to PD, such as constipation and REM-Sleep Behavior Disorder (RBD), effectively evading diagnosis based on current diagnostic standards (Mantri & Morley, 2018). This latent and early stage of PD has been named Prodromal-PD and is defined by Mantri and Morley (2018) as "the stage at which individuals do not fulfill diagnostic criteria for PD…but do exhibit signs and symptoms that indicate a higher than average risk of developing motor symptoms and a diagnosis of PD in the future".

Parkinsonian Rigidity

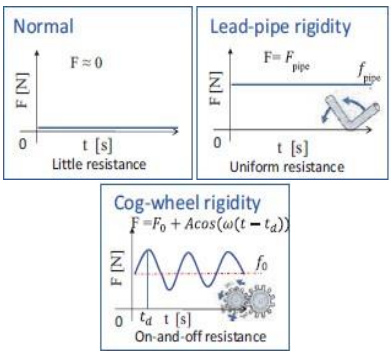

Figure 2: Types of Rigidity (Wang et al., 2014)

Though each patient will experience many non-motor and motor symptoms, the most associated and diagnostically relevant symptoms caused by the death of these neuronal cells, are movement related, including tremor, rigidity, and bradykinesia (Guttman & Furukawa, 2003). Joint rigidity, one of the key indicators, results from the inability of the muscles to relax and extend properly due to an increase in passive stiffness of the affected muscles brought on by reduced levels of dopamine (Cano-de-la-Cuerda et al., 2011). An increase in passive muscle stiffness can cause two different types of rigidity, lead-pipe rigidity and cogwheel rigidity (Endo et al., 2009). Lead-pipe rigidity is detected as a constant force and defined as uniform resistance, while cog-wheel rigidity is detected as an intermittent force and defined as on-and-off resistance shown in Figure 2 (Chunbao Wang et al., 2014). Rigidity, regardless of the type, often begins in one arm and gradually spreads unilaterally to the leg, then through the trunk and eventually to the other side of the body and is not always present during passive movement but can be brought on by movement on the contralateral side of the patient such as opening and closing the patient's hand, known as Froment's Maneuver (Association, E. P. D., 2016; Guttman & Furukawa, 2003).

Clinical Standard for Rigidity Assessment

The current standard for assessing rigidity in a clinical setting is a subjective test completed by the clinician on the arm of the patient. This exam relies on the clinician to determine whether the level of rigidity has increased based on the feel of the relaxed wrist and elbow joints as they perform passive flexion and extension (Perera et al., 2019). Rating the perceived degree of rigidity during this exam and comparing it to prior visits to determine if the perceived degree of rigidity has changed does not allow for an accurate measure of rigidity, which can be made worse if the patient is experiencing tremors or cog-wheel rigidity at the time of the exam, and lacks repeatability due to uncontrollable external factors. Due to the varying rates at which rigidity develops from one patient to the next and the lack of reproducibility

of the diagnostic exam, the level of rigidity and progression of this critical PD symptom cannot be quantitatively measured. The presence of quantitative data regarding progression of rigidity could lead to more customized drug treatment options and an eventual increase in Health-Related Quality of Life (HRQoL).

Diagnosing PD

Because of the variability and unpredictability of its symptoms and the overlap of symptoms with other neurodegenerative disorders, a phenomenon described by the term Parkinsonism, PD can be difficult to diagnose and treat effectively. In addition to the erratic nature of symptom presentation and progression, the only definitive diagnostic test is one implemented post mortem and there are currently no objective clinical measures of disease progression (Guttman & Furukawa, 2003; Merello & Antonini, 2019; Bhidayasiri, & Martinez-Martin, 2017). Because of this, much of the past PD research has been dedicated to creating, testing, and improving subjective measures, while proposing and testing objective measures for diagnosing and evaluating disease progression.

Clinical Standard for Diagnosis

The current clinical standard for diagnosing and determining approximate disease progression is a combination of three parts, including: a complete neurological evaluation, in which the neurologist will assess affected motor controls watching for any issues with gait, balance, and muscle tone; an in-depth review of the patient's medical history, including any prodromal symptoms; and subjective disease surveys completed by the patient and clinician (Ford-Martin & Alic, 2005; Holden et al., 2018; Downward, 2017). In an attempt to mimic the diagnostic process of expert clinicians and develop a standard for those who have less experience, the Movement Disorder Society (MDS), created a diagnostic tool aptly named the Movement Disorder Society Clinical Diagnostic Criteria for Parkinson's Disease (MDS-PD Criteria). This guide was designed for use in research, but upon further testing, the MDS observed high sensitivity and specificity of the criteria when compared with the current gold standard –

diagnosis by an expert. This confirmed the diagnostic capability labeling the MDS-PD Criteria as a valid clinical diagnostic tool (Postuma et al., 2018).

MDS-PD Diagnostic Criteria

The MDS-PD Criteria explains that after motor Parkinsonism existence is determined, with help from the MDS-UPDRS and defined by the presence of bradykinesia (the core feature of clinical PD) accompanied by either rigidity, resting tremor or both, a PD diagnosis can be determined based on three categories of diagnostic features. Feature 1 – absolute exclusion criteria (a negative feature that argues against PD diagnosis) is meant to rule out PD from other parkinsonisms; feature 2 – red flags (another negative feature which must be offset by supportive criteria to allow diagnosis), and feature 3 – supportive criteria (a positive feature that increase confidence of PD diagnosis) (Tysnes & Storstein, 2017; Postuma & Berg, 2016). From these features there are two levels of diagnostic certainty: clinically established PD and clinically probable PD. The requirements for the diagnosis of each are shown in Table 1. Clinically established PD maximizes specificity, providing a reliable diagnosis when the test is positive but not necessarily ruling out the disease when the test is negative. Whereas, clinically probable PD balances specificity and sensitivity, considering more of the false negatives that high levels of specificity neglect (Postuma et al., 2015).

Table 1: MDS Clinical Diagnostic Criteria for Parkinson's Disease (Postuma et al., 2015)

Type of diagnosis	
Clinically Established PD	Clinically Probable PD
1. Absence of absolute exclusion criteria	1. Absence of absolute exclusion criteria
2. At least two supportive criteria	2. Presence of red flags counterbalanced by supportive criteria. If 1 red flag is present, there must also be 1 supportive criterion.
3. No red flags	No more than 2 red flags are allowed in this category.

Subjective Rating Scales

After a diagnosis is made, tests are conducted to determine approximate disease progression. Rigidity along with other PD symptoms are evaluated subjectively in three prominent rating scales, the

Movement Disorder Society's – Unified Parkinson's Disease Rating Scale (MDS-UPDRS), the Hoehn and Yahr Scale (H&Y), and the Parkinson's Disease Questionnaire-39 (PDQ-39) (Ford-Martin & Alic, 2005; Holden et al., 2018; Downward, 2017; Bhidayasiri, & Martinez-Martin, 2017).

Movement Disorder Society's – Unified Parkinson's Disease Rating Scale

The MDS-UPDRS is a comprehensive ordinal rating scale created in the 1980s and revised by the MDS in 2008 to reflect research and advances made since its creation (Goetz et al., 2008). The goal of this rating scale was to provide an easy to use, comprehensive rating scale that would work for all PD patients regardless of disease severity, current medications, or age. Proven through clinimetric testing to be a reliable and valid tool for all stages of PD diagnosis and progression, the MDS-UPDRS has four distinct parts, encompassing both motor and non-motor symptoms of PD. The four parts are Non-Motor and Motor Experiences of Daily Living (NM-EDL, M-EDL), Motor Examination, and Motor Complications. Each question has 5 possible answers relating to frequency or intensity, ranging from 0 (normal) to 4 (severe) (Goetz et al., 2008). The MDS-UPDRS is administered by a combination of a clinician and the patient or caregiver, if necessary, depending on the section.

Hoehn and Yahr Scale

The H&Y scale is used to characterize progression of motor symptoms on a scale of 1 – 5 but does not account for non-motor symptoms of PD (Barmore, n.d.). The H&Y scale, administered completely by the rater, consists of five stages used to demonstrate the overall disease progression as defined by the patient's approximate level of disability (Goetz et al., 2008; Bhidayasiri, & Martinez-Martin, 2017). Stage I of H&Y is considered early disease in which the patient experiences mild, unilateral PD symptoms with minimal to no effect on function; Stage II is still considered early disease like Stage I but includes bilateral symptoms and possibility of experiencing problems with speech, rigidity, tremor, and bradykinesia; Stage III, considered mid-stage, is characterized by postural instability, with falls becoming increasingly common, bradykinesia, and the ability of the patient to remain fully

independent; Stage IV progression is severe and patients are noticeably incapacitated and unable to live independently, needing some assistance in daily activities; Stage V describes a patient who is wheelchair or bedridden, needing 24-hour assistance, and possibly experiencing hallucinations (Downward, 2017). The ease of use and clear result of the H&Y have caused it to become a commonly adopted metric for describing a patient's PD stage throughout the progression of the disease (Bhidayasiri, & Martinez-Martin, 2017); the patient's H&Y rating is even included as a question in part three of the MDS-UPDRS (Goetz et al., 2008).

Parksinson's Disease Questionnaire - 39

The third and final subjective measure, the PDQ-39, evaluates the effects that PD has on the patient's Health-Related Quality of Life (HRQoL). This test is made up of 39 questions, completed by the patient with multiple choice answers, regarding frequency of symptom manifestation, ranging from 0 (never) to 4 (always). As a measure of HRQoL and well-being, the PDQ-39 focuses on the impact that PD has on the mental state, emotional state and the level of social functioning of the patient (Cano-de-la-Cuerda et al., 2011; Health Related Quality of Life and Well-Being, 2010).

These subjective measurements have been generally successful at diagnosing PD and determining approximate disease severity because de novo diagnosis of PD and qualitative measurement of disease progression are both based on symptoms that can be subjectively assessed by the patient and the clinician (Guttman & Furukawa, 2003).

Objectives

While the subjective scaling systems currently in use have proved their efficacy in determining overall disease progression of PD and will remain valuable assets in research and diagnostic efforts, it is well known that quantification of disease state, including progression and severity of individual symptoms like rigidity, is a necessity when it comes to PD monitoring and research. In these rating scales

the information provided by the patient and the clinician is subjective and can change based on various human and environmental factors present on the day the survey is administered (Guttman & Furukawa, 2003). However, studies show objective quantification of rigidity can be achieved by determining the amount of torque needed to change passive joint position during externally imposed movement (Xia et al., 2010). PD's variability necessitates quantifiable objective measures in order to obtain unbiased results, detect subtle changes in symptom progression, and simplify patient participation in future studies to better understand the mechanisms of rigidity in parkinsonian disorders (Bhidayasiri & Martinez-Martin, 2017). The goals of this study are to develop a torque-based device, using a servo motor, that will objectively measure rigidity in the arm of patients suffering from PD and other movement disorders, to incorporate necessary hardware-based safety features for safe operation and characterize the device to determine its suitability for use in future research endeavors.

II. Previous Attempts

Motivation

Parkinson's Disease progression, currently evaluated by subjective clinical scales, is monitored and reported in terms of disease progression as a whole and not individual symptom progression. As a result, inter-patient variability of symptom manifestation and progression is a known drawback of diagnosing and tracking PD. As such, objectively quantifying rigidity, one of the cardinal features of PD, would be useful for evaluating symptom progression, ultimately increasing treatment efficacy and resulting in a better QoL. Rating scales, as the backbone of clinical standard for diagnosis, are limited by their subjectivity. Since the mid-1900s there have been many attempts at objectively quantifying rigidity but limitations, including lack of correlation with current rating scales and small sample sizes, have prompted the absence of a clinically accepted standard (Prochazka et al., 1997). Recent research on the quantification of rigidity has been focused on producing mechanical devices, equipped with sensors to measure torque, angular velocity, and other variables during passive movement, for objective

quantification. These mechanical devices can be delineated into two categories, rater-driven sensor devices, and power-driven sensor devices which incorporate a drive such as a servo motor.

Rater-driven Sensor Devices

Before 1997, many methods were attempted using sensors to quantify rigidity however, Prochazka et al. noticed that there were major differences between these methods and the standard clinical exam. In their 1997 study, the clinical exam was completed on subjects while equipped with a force sensing cuff and transducers to measure force and displacement gauge to measure changing position. Torque (or limb impedance) was then calculated by multiplying the distance between the point of application of the sensor and the elbow joint by the force. This study was completed on 14 patients with mild to severe PD and the results were compared to the UPDRS at the time of the study. The subjective rating of rigidity was determined for each patient by the clinician before the tests were performed a second time with the cuff. The authors found that rigidity varied greatly during the clinical exams monitored by the cuff but that during the standard clinical exam, a single number associated with rigidity is given. As a result, this did not allow for accurate comparison between the clinical exam occurring with and without the cuff. To avoid this limitation, during the exam with no cuff, the rater continually verbalized their estimated rigidity rating. In this study there were observed differences in the speed and range at which raters performed their tests but no statistical difference in the mean impedance between raters was found, indicating that rater variability was not an issue. However, this study also examined rigidity in the patient when on and off medications but found that while the calculated torque values were different, the values perceived by the clinician were not, suggesting that the score of the rater was not always a reliable assessment of rigidity. Because of the exclusion of the many influences of limb rigidity in engineering tests, not only did this study conclude that "narrowing down" of test conditions using this or other devices is contradictory to the clinical exam but also concluded that a simple device such as this would allow for increased inter-rater reliability.

In a similar study by Takayuki et al., in 2009, torque was calculated after measuring force with a series of force sensors and a gyroscope, and distance from the elbow joint during passive flexion and extension movements; however, EMG data was also collected, to analyze any myoelectric features during passive movement of the limb. This study had a sample size of 51 patients, consisting of 24 healthy older adults and 27 PD patients with rigidity ranging from mild to moderate and rated each patient using the MDS-UPDRS before any testing was completed. A hold-ramp-hold-ramp-hold movement was implemented starting at maximum flexion to determine muscle tone during flexion and extension. The authors found that rigidity values based on the calculations of torque did not correlate well to the UPDRS because the muscular dynamics of rigidity differ between flexion and extension, further demonstrating the limitations of the current clinical procedure. As a result, the authors defined rigidity as a sum of an "elastic" component and average force which they termed "difference of bias" and noted that the most studies do not differentiate between flexion and extension scores during testing.

Ultimately the authors in both studies noted that further study was needed to determine how to mimic current clinical standard exams in a controlled environment while monitoring all test parameters including muscle tone during passive flexion and passive extension.

Power-driven Sensor Devices

Each of these studies considered subjective testing an insufficient tool to monitor changes in rigidity and considered the quantification of rigidity important for determining and increasing efficacy of drug treatment methods. The basis of the device used to measure rigidity by Relja, Petravic, and Kolaj (1996) is an electromotor that drives an "arm board" equipped with a torque transducer and a potentiometer used to simultaneously measuring torque and position, with a constant velocity, through phases of passive flexion and extension. "Net work" was calculated as a measurement of rigidity and represented by the area of a hysteresis diagram. Each of 127 subjects, made up of 24 PD patients and 103 controls, was evaluated using the UPDRS before the trial. The authors also measured rigidity with respect to activation of the contralateral limb known as activated rigidity when patients were on and off

medications to determine differences before and after treatment. The study was deemed repeatable, and clinically reliable when compared to subjective ratings of rigidity. In spite of this, the small sample size of PD patients and comparatively limited disease knowledge were the main limitations of the study.

In a 2002 study by Powell et al., the authors sought to determine the effects of velocity and amplitude on rigidity during passive movement and to determine the effects of dopaminergic medications on rigidity. The device used in this study consisted of a servo motor and shaft attached to the end of a manipulandum. Torque and position were measured about the wrist during ramp and hold trajectory for four different combinations of velocity and angle of displacement. Surface EMG was also measured on the wrist and finger flexor muscles for each patient. The initial measurement occurred when patients were off medication for at least 12 hours and then tests were completed again after their normal dose was administered. Hysteresis curves of torque with respect to joint position were analyzed along with EMG data. The authors found that the greater the angle of displacement, the greater the value of rigidity, determining that rigidity is dependent on amplitude though the this contradicts the clinical description of rigidity as constant passive stiffness. These authors also found that rigidity did not significantly decrease due to dopaminergic medication however a major limitation is the single orientation in which this study measured rigidity compared to the three-dimensional movements assessed in clinical exams.

Together, these studies explore only a few of the causes associated with and tests quantifying and treating parkinsonian rigidity. Small sample sizes, a lack of correlation with clinical standards and clinical testing procedures, and lack of complete joint modeling are just a few of the hurdles necessary to overcome to objectively quantify joint rigidity.

A third study (Sin et al., 2019), used a robotic device to improve repeatability, and inter-rater reliability while measuring spasticity in stroke patients during stretch reflex measurements. While spasticity is not the same as rigidity, the device design is relevant and is composed of a torque sensor, a processor, an encoder, a motor, a controller and a forearm manipulandum style arm sling. The arm sling uses linear sliders to perfectly adjust the length from the axis of rotation to the manipulandum handle and position of restraints to fit each individual patient and to ensure that the elbow is aligned about the axis of

rotation. In this study, the adjustable arm sling allows for repeatability in testing and the controller allows for inter-rater reliability. Adopting the concept of creating an adjustable arm sling would allow for increased inter-rater reliability and thus repeatability while measuring torque.

III. Methods

Device Setup

To quantify rigidity, a torque-based device was designed to be used on a patient's arm. The device consists of three key inter-connected components (Figure 3). The first, called the motor assembly, utilizes a 20KΩ, heavy-duty, multi-turn, precision potentiometer (Bourns, 3540S-1-203L) to measure shaft position of the servo motor (Kollmorgen, JR16M4CH/ENC), a transmission-shaft assembly, equipped with a torque transducer (Sensotec, QSFK-9/J301-01) to measure torque, two photologic slotted optical switches (TT Electronics, OPB991) to limit the angle of rotation, and a rigid forearm sling. The connections of this assembly run through an emergency power shut-off junction box for organization of electrical connections and added safety. The second component, called the controller/power assembly contains data processing components and the power supply components of the device including a transducer power supply (Transducer Techniques, Model PSM-R), a 12000 µF electrolytic capacitor

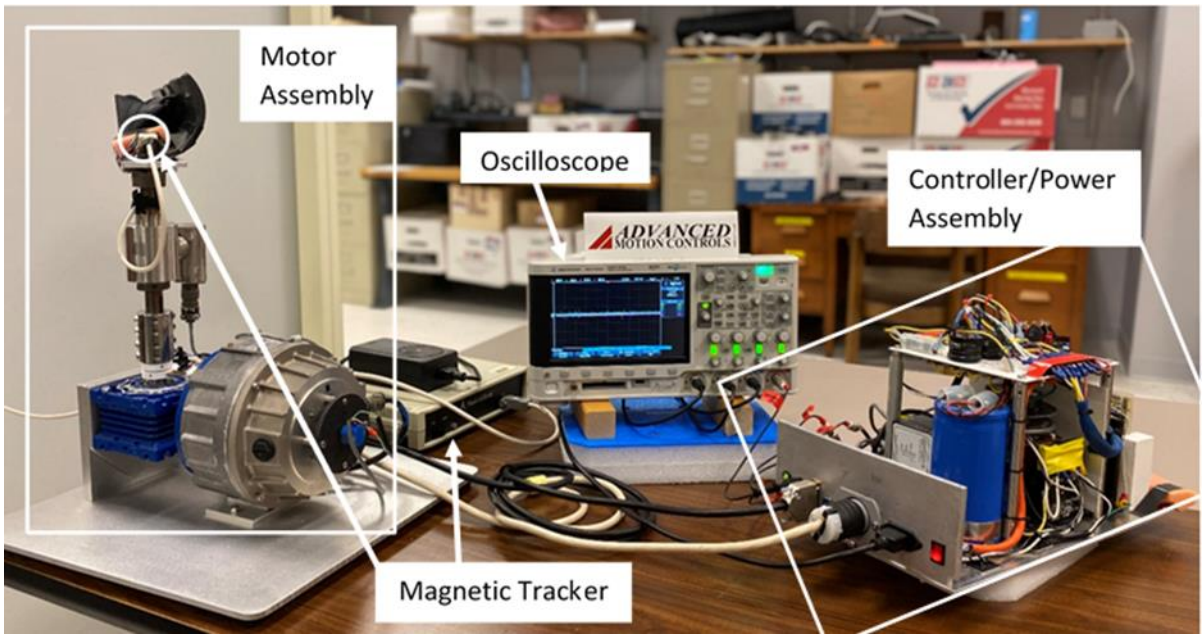

Figure 3: Device Setup (not pictured: computer, D/A, and A/D converters)

(Vishay Sprague Powerlytic™, 36DY), Variac transformer (Staco, 1010B), servo amplifier/controller (Advanced Motion Controls, 25A20), 12V DC power supply, and safety circuit board. The two compartments are connected via a DB-15 connecter cable in order to provide the device's input and output signals, and a locking power cable to power the motor. The third assembly consists of the external data processing equipment including an analog-to-digital (A/D) and a digital-to-analog (D/A) converter, a computer, and an oscilloscope (Agilent Technologies, DSO-X 2024A) used for viewing real-time data. An isolation transformer (Toroid, ISB-060A) is used to avoid ground loops and isolate the common ground for the device and power ground from the outlet. A full list of parts can be found in Appendix 1. The connections between and within these components can be seen in Figure 4 and Figure 5. Using an MS DOS computer platform, stimulus signals are sent through the controller/power assembly to the motor while position and torque data are sent through the controller/power assembly to the computer

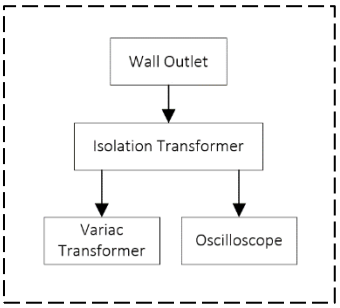

Figure 4: Isolation Transformer Block Diagram

Figure 5: Device Block Diagram

simultaneously. Working together, these three components flex and extend the elbow joint to mimic the movements during rigidity testing in the current standard clinical setting and the combination of position and torque data are used as a measurement of rigidity with respect to time.

Features of the Motor Assembly

The motor assembly, shown in Figure 6, consists of several components that drive the motor and track torque and position during each experiment. The servo motor is the basis of the assembly and allows for precise control of rotation. Attached to one end of the motor is the multi-turn potentiometer, which monitors lateral position of the patient's arm. The output of the potentiometer is an analog signal directly correlated to position with respect to time. Attached to the opposite end of the motor is the transmission-shaft assembly, which can rotate 90° to allow for measurement of torque about the horizontal or vertical axis. Two optical switches are affixed at the base of the shaft on the transmission to a 3D printed mount that allows for different heights of the two sensors. These sensors work in conjunction with two 3D printed shaft collars with attached brass vanes. The printed shaft collars contain small set screws that allow for positional adjustments of the collars and vanes. The maneuverability of the shaft collars allows for restriction of the angle of rotation of the rigid arm sling as a safety precaution (more information is included in Hardware Safety Features). The torque transducer is located towards the top of the shaft to measure torque as the shaft rotates and the rigid forearm sling is affixed at the top of the shaft, with its axis of rotation about the shaft. The output voltages of the potentiometer, torque transducer, and two optical switches and power inputs for the torque transducer, optical switches, potentiometer and servo motor are all fed through a plastic

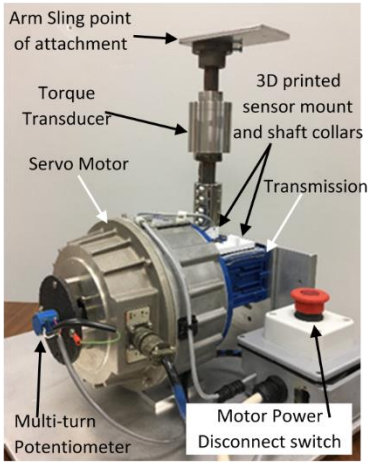

Figure 6: Motor Assembly (not pictured: mounted optical switches, DB-15 inter-assembly connector)

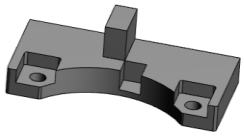

Figure 7: 3D model of the photologic optical switch mount

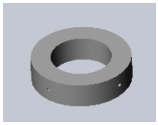

Figure 8: 3D model of a shaft collar

junction box equipped with a red emergency power shut-off button which when pressed disconnects power to the motor and must be twisted in order to be released.

Controller/Power Assembly

The controller/power assembly contains data processing components and the power supply components of the device including a transducer power supply, 12000µF electrolytic capacitor, Variac transformer, servo amplifier/controller, 12VDC power supply, and safety circuit board. The transducer power supply is a bipolar supply that powers only the torque transducer. There is also an isolated 12VDC power supply that is used to power the TTL safety circuit board. Separate power supplies are needed because the safety circuit and torque transducer together exceed the current limits of the transducer power supply. However, it is important to note that all ground signals within this device are common, including the chassis, to avoid ground loops. The Variac transformer, motor supply circuit, and transducer power supply provide power to the servo motor and torque transducer. The servo amplifier/controller is designed to drive DC motor with precision and is one of the most important components because it controls the motor. Using a negative feedback loop the controller analyzes the position of the motor with respect to the position of the input stimulus. If there is any difference between the two signals >~100mV, the servo motor, driven by the shaft position difference with the motor, produces a step change in position to minimize the error. These movements are intense, jolting movements and while not unsafe, they can be uncomfortable. For this reason, the position of the sling should be adjusted so that the potentiometer signal and stimulus signal are equal before the inhibit is reset. The output of the safety circuit is also

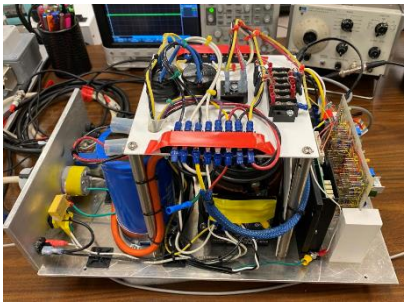

Figure 9: Controller/Power Assembly front view

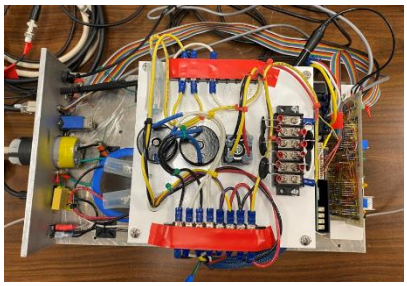

Figure 10: Controller/Power Assembly top view

Figure 11: Controller/Power Assembly rear view

monitored by the controller using the inhibit feature. This feature is used to implement limits that when triggered will shut down the motor by pulling the inhibit signal to ground. Under normal and safe conditions, the output of the safety circuit to the inhibit pin is 5V. In accordance with the safety circuit, when unsafe conditions are met, the output of the circuit drops to 0V and stays there until the device is the device is reset, causing the controllers inhibit to trigger.

Hardware Safety Features

To ensure the safety of any participant, a transistor-transistor logic (TTL) based digital safety circuit was designed using integrated circuits to interact with the inhibit feature on the controller. All connections were installed onto a circuit board using a combination of solder and wire wrapping, a technique that produces connections more durable than those made strictly with solder and allows for more simple modifications. When the inhibit signal on the controller is pulled to ground (0 volts), the controller cuts power to the motor. To make this device safe, we incorporated three limits into the circuit design, position, velocity and torque.

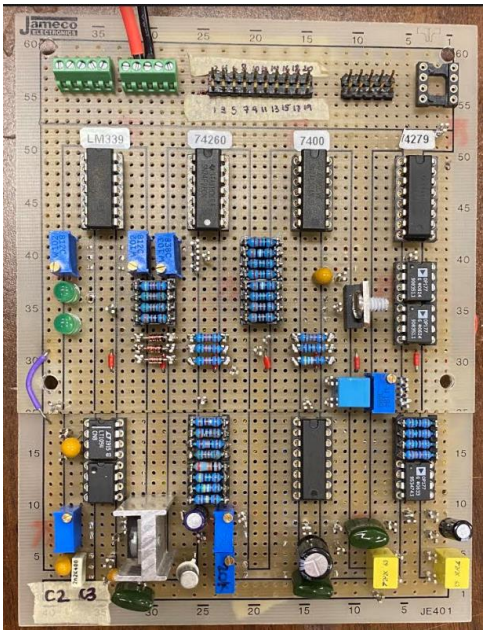

Figure 12: Safety circuit board (front view)

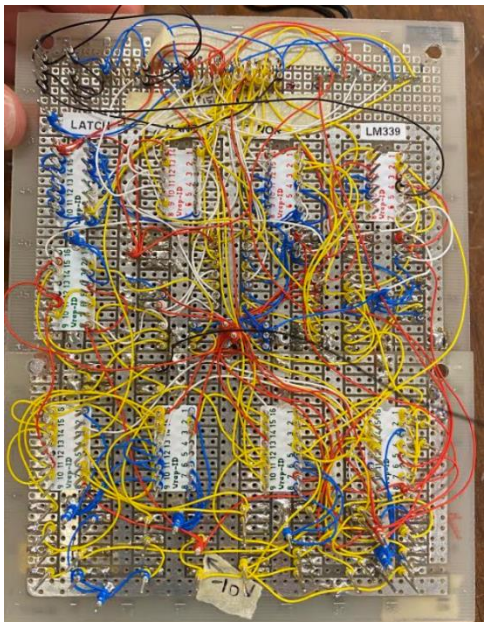

Figure 13: Safety circuit board (back view and wire wrap connections)

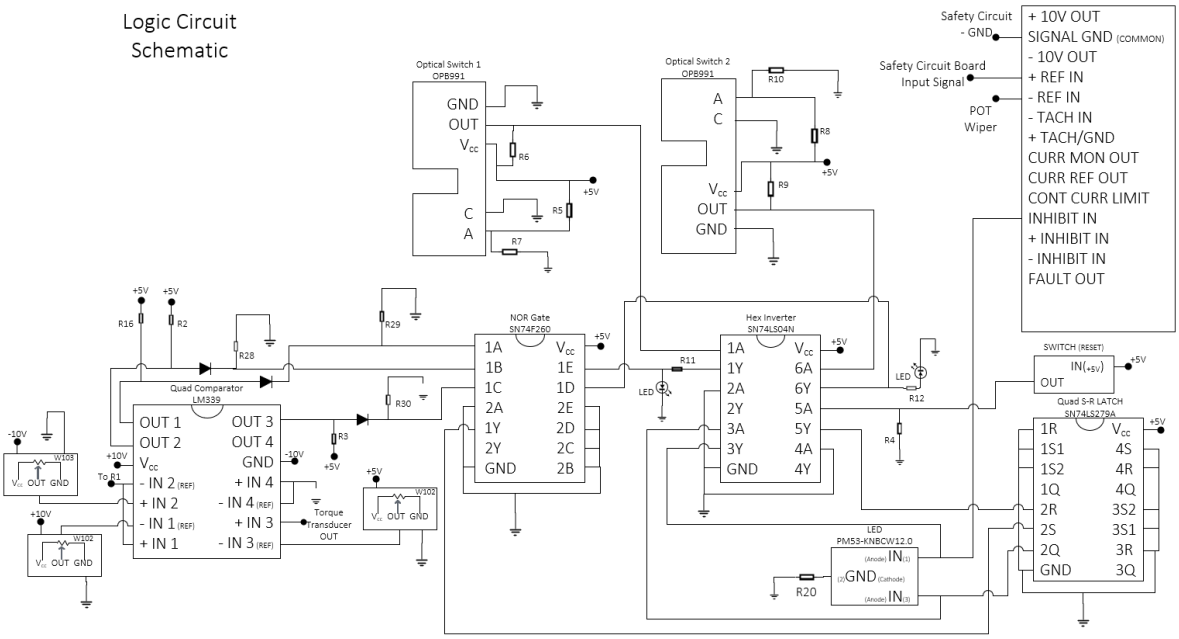

Figure 14: Logic Circuit Schematic

Position Limit

The position limit (Figure 15) restricts shaft angle of rotation and includes two photologic slotted optical switches mounted at the base of the shaft and two shaft collars, with brass vanes attached, tightened onto the shaft using set screws. During testing, the shaft collars were set to ensure that the rigid arm sling would not rotate more than 90° but can be adjusted to desired angle. As the shaft rotates, the vanes of brass rotate with the shaft. When either vane passes through the slot of an optical switch, interrupting the signal, the output of that optical switch drops to 0 volts(V), known as logical LOW. A hex inverter (Texas Instruments, SN74LS04N) was used to invert the logic signal of the optical switches so they would match

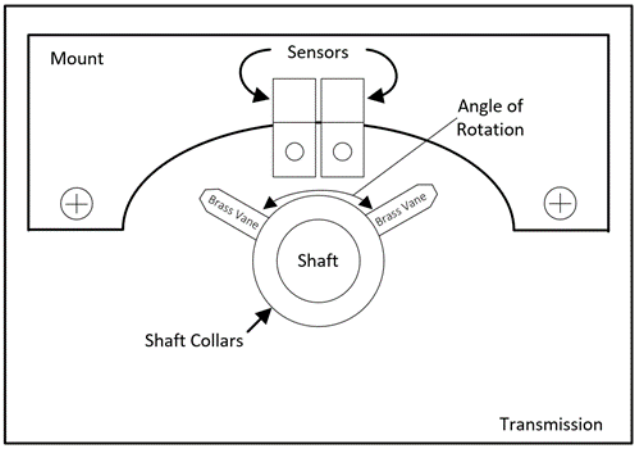

Figure 15: Visual representation of the position limit viewed from above transected shaft.

the logic of the quad differential comparator (Texas Instruments, LM339) which goes to 5V, or logical HIGH, upon exceeding its limit.

Torque and Velocity Limits

Three comparators on a quad comparator chip were used to evaluate limits set for velocity and torque. Position data from the potentiometer was differentiated using a High Pass Filter (HPF) (Figure 16) to attain velocity and amplified to counteract the effects of the HPF on the signal. These values of velocity were compared to reference values using the comparator. The torque values from the torque transducer were also passed through the comparator. Because the potentiometer is bi-directional, the values received from the potentiometer are both positive and negative and must be analyzed as such. The TTL logic of the comparator states that if input voltage (V_{in})>reference voltage (V_{ref}) the output is a logical 1 or 5V (HIGH), whereas if $V_{in}<V_{ref}$ the comparator output is LOW. Standard comparator logic does not work for negative values, so we created a window comparator that allows for the comparator to

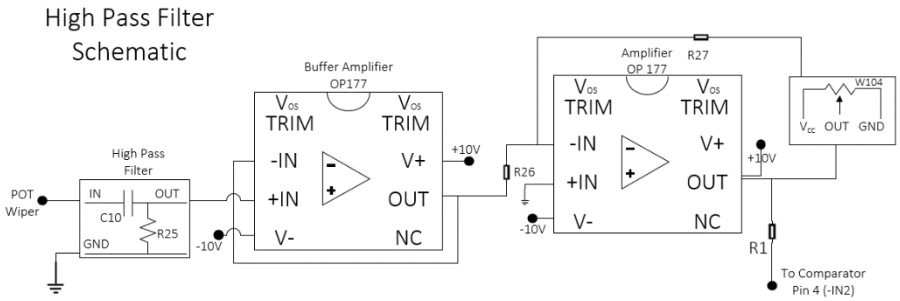

Figure 16: High Pass Filter Schematic

judge based on a reference window instead of a single reference value. If the source signal is between the two reference values (within the window) the output is LOW, but if the source signal falls outside of the reference signal the comparator output goes HIGH.

Position, Torque, and Velocity Create the Inhibit Signal

Next, all three outputs of the comparator are sent to a dual 5-input positive-NOR gate (Texas Instruments, SN74F260) which evaluates inputs based on the NOR logic (Figure 17) and combines them into one output; if any input is high the output of the NOR is LOW. The inverted signal from the optical switches is also sent to the NOR gate so that if any one of these devices is tripped (HIGH), the output of the NOR is LOW. The signal output of the NOR matches with the logic of the inhibit pin but a latching mechanism was needed in order to make sure the device turned off and stays off instead of turning back on as soon as the error is resolved. To achieve this, a quadruple set-reset (S-R) latch (Texas Instruments, SN74LS279A) was used along with a single pull, single throw (SPST) always off-momentarily on (OFF-MOM) push button switch (Grayhill) and a 3-lead bi-color LED (Bivar, PM53-KNBCW12.0) indicator light which turns red if the inhibit signal has been tripped and stays green at all other times. The output of the S-R latch (which stays latched until manual reset, Figure 18) is sent to the controller as the input for inhibit. When the inhibit feature is active (meaning there is an issue), the indicator light will be red, the motor will be off, and the push-button switch will have to be pushed just once in order to reset.

inputs		output
A	B	Y
0	0	1
0	1	0
1	0	0
1	1	0

Figure 17: NOR Logic
(http://www.eeherald.com/section/design-guide/logic-design.html)

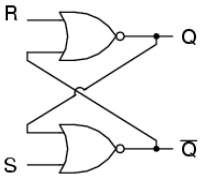

S	R	Q	$\overline{Q}$
0	0	latch	latch
0	1	0	1
1	0	1	0
1	1	0	0

Figure 18: Set-Reset Latch Logic. Output = Q
(https://www.allaboutcircuits.com/textbook/digital/chpt-10/s-r-latch/)

Additional Components of the Safety Circuit

In addition to the logic components of this circuit, there are several others necessary for the safety circuit to work. These include the negative voltage converter (Figure 19), which converts a +12V into -10V to be used as Vin for several of the devices using a switched-capacitor voltage converters with regulators (Texas Instruments, LT1054), the adjustable linear voltage regulator (STMicroelectronics, LM317T) (Figure 20), which regulates 12V down to 10V, the five volt fixed voltage regulator (Texas Instruments, LM340T) (Figure 21), and the high pass filter (Figure 16), needed to differentiate and analyze the position data. Together these TTL devices form the hardware-based safety features for this device.

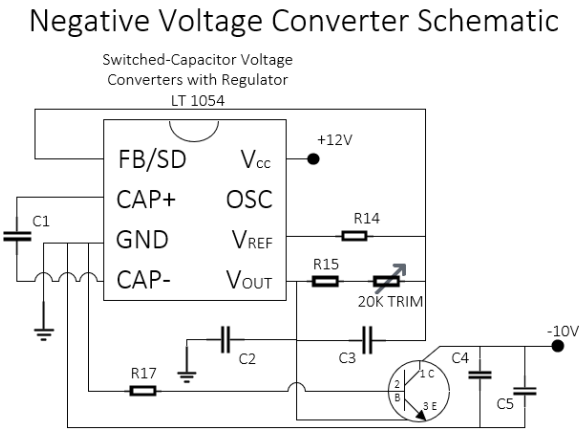

Figure 19: Negative Voltage Converter Schematic

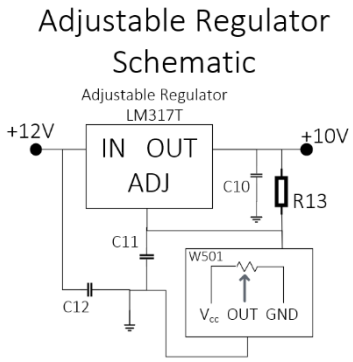

Figure 20: Adjustable Regulator Schematic

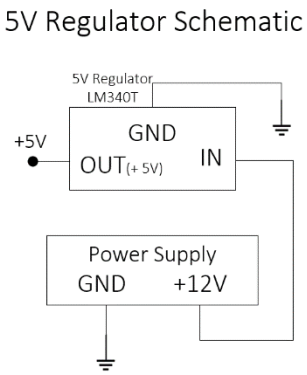

Figure 21: 5V regulator Schematic

Data Processing Assembly

The software used for processing the data was software created and modified by Dr. Paul Wetzel using a MS DOS platform in line with an external A/D and D/A converter. The program provided stimulus files to the controller and the A/D sampled the potentiometer and torque data each at a sampling rate of 500Hz. Because these stimulus files were created for a different use, we attenuated the ramp and sine files using an external potentiometer.

Connections Between Assemblies

A DB-15 cable was used to make each connection from the motor assembly to the controller/power assembly aside from the power cable for the motor which was connected with an industrial grade non-shrouded locking plug to ensure that the motor would not become disconnected from power by mistake. Device signals were sent to and from the controller/power assembly and the data processing equipment with BNC cables.

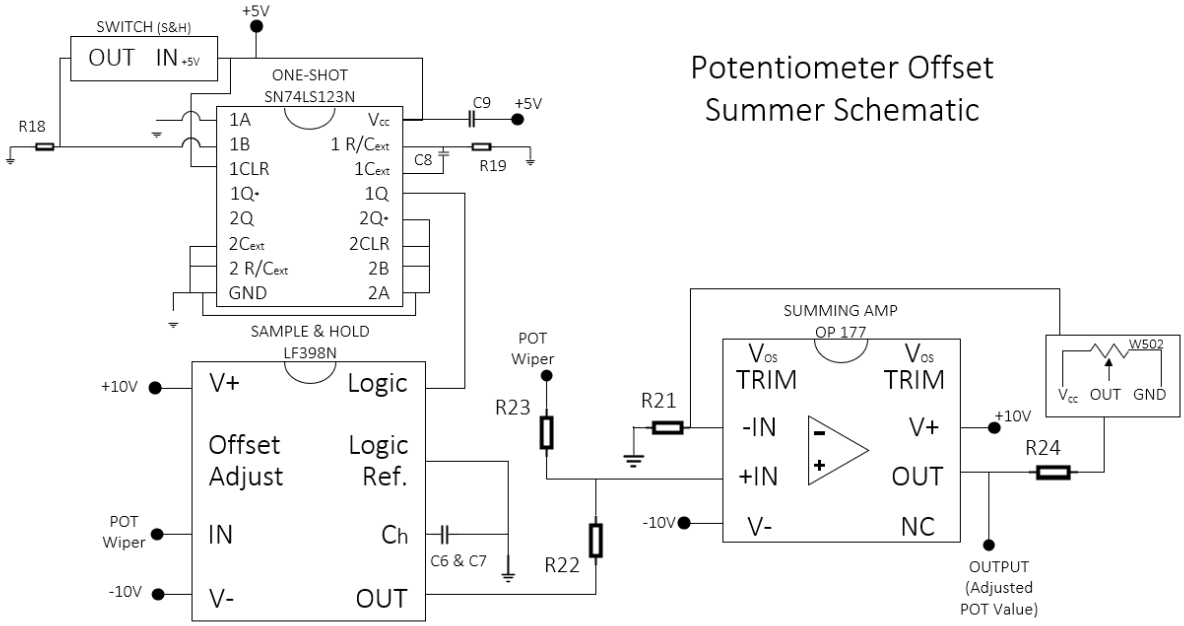

Figure 22: Potentiometer Offset-Summing Amplifier Schematic

Participants

In lieu of the restrictions due to the COVID-19 pandemic, no PD patients were available, and no study was able to take place. Instead, evaluation was completed on two healthy individuals, person 1 and person 2, identified by GM and PW, respectively. To simulate a scenario with increased torque, as is the case with Parkinsonian rigidity, individuals were instructed to co-contract the muscles surrounding their elbow joint by clenching the fist of the tested arm. Tests were run on the right arm of each participant.

Evaluative Protocol

Person 1 and person 2 were instructed to stand perpendicular to the table next to the device, with their right hip touching the side of table. The individual's right arm was then placed in the sling with their elbow sitting directly over top of the shaft and their palm positioned outward with their thumb toward the ceiling. The arm was secured with two Velcro straps, one at the wrist and one just below the elbow, to restrict movement of the arm within the sling. The position of the rigid arm sling was then moved to the zero position, as seen on the oscilloscope, by rotating the shaft until the position signal on the scope matched that of the stimulus signal; in this case the stimulus file was programmed so that it started and ended the signal at zero volts. The zero position of the potentiometer correlated to a flexion angle of approximately 45° about the elbow. This setting can be altered by turning the potentiometer by hand and should be decided upon based on the content of the stimulus file, for example, when using a sine wave, which oscillates above and below zero periodically, you must start the device in the center of the range of motion.

Directions were given to the individual to relax their limb as much as possible during relaxed tests and make a tight fist during the entirety of the co-contraction tests. Three stimuli were applied including, sinusoidal stimulus (sine3.dat), a ramp stimulus (ramp3.dat), and a random stimulus (rnd-100f.dat) made up of sinusoidal content of varying amplitude and frequency. The forearm was displaced through a maximum total range of 90° (+/- 45° from the zero position). Each person underwent two trials of each stimulus type, one with a relaxed joint and one under co-contraction. Each stimulus file was also run with no load to determine the level of device noise for each test. Data from the torque transducer and potentiometer were sampled at a rate of 500 Hz. Using a stand-alone six degree of freedom magnetic tracking system called, A Flock of

Figure 23: Arm shown during relaxation

Figure 24: Arm shown during co-contraction or clenched-fist phase

Birds (Ascension Technologies, Colchester, VT), angle (yaw, pitch, and roll) and position (x, y, z) data was also collected at a rate of 125 Hz and expanded to 500 Hz, by repeating each value four times, to allow for comparison between the files and to determine the degree of yaw, pitch and roll of the device arm.

Data Analyses

Torque and position output voltages for relaxation and co-contraction evaluations were graphically compared with respect to time for each different stimulus. Mean and variance were also calculated for torque in each trial and compared to one another within their stimulus category. Using a custom code written by Dr. Paul Wetzel, Discrete Fourier Transforms were performed on the torque data to determine the frequency content of the random and sine stimuli.

IV. Results

Comparison of Velocity to Stimulus Position

To determine efficacy of the HPF, the velocity was sampled instead of torque during a test run of the random stimulus with no load. In the graph of velocity and position with respect to time, shown in Figure 25, we expected to see the velocity curve, shown in red, phase shifted to the right of the stimulus file. This graphical representation proves that the HPF is differentiating position into velocity.

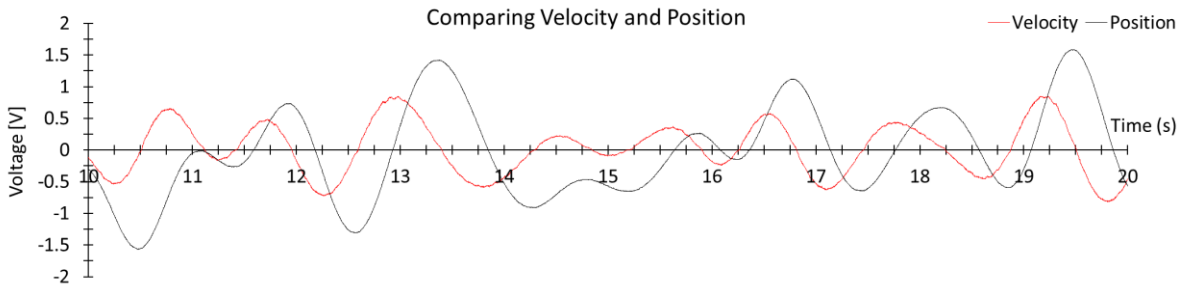

Figure 25: Values for position and velocity with device under the "no-load" condition.

Quantification of Perceived Rigidity in Co-contracted Versus Relaxed Trials

Perceived rigidity during co-contraction and during relaxation was compared for each person and for each stimulus signal. During the relaxed tests for sine (Figure 32 and Figure 34) and random stimuli (Figure 27 and Figure 29), the torque values are relatively low with a couple of peaks following significant changes in the stimulus. During the co-contraction tests for sine (Figure 33 and Figure 30) and random stimuli (Figure 28 and Figure 30), the peaks are larger meaning that perceived torque is greater during the clenched-fist phase than during the relaxed phase. This makes sense based on prior research. During the ramp stimulus, there is not a significant difference between torque during co-contraction (Figure 38 and Figure 40) and during relaxation (Figure 37 and Figure 39). Median torque and variance were also calculated for each test resulting in exceptionally low variances (Table 2, Table 3, and Table 4).

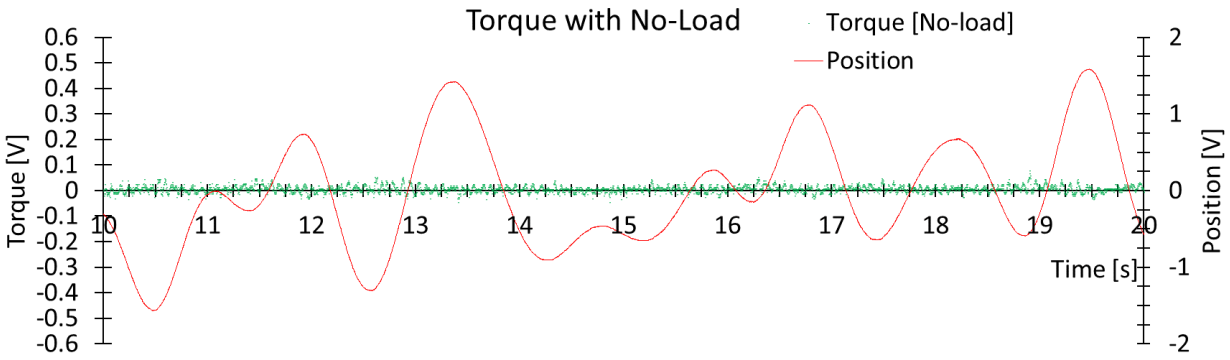

Figure 26: Torque values for the Random stimulus with no load.

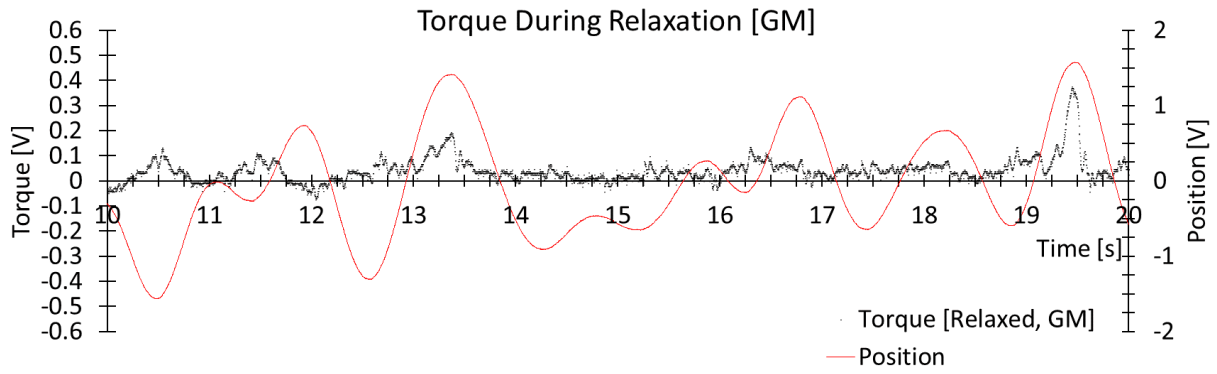

Figure 27: Torque values for the Random stimulus during relaxation for GM.

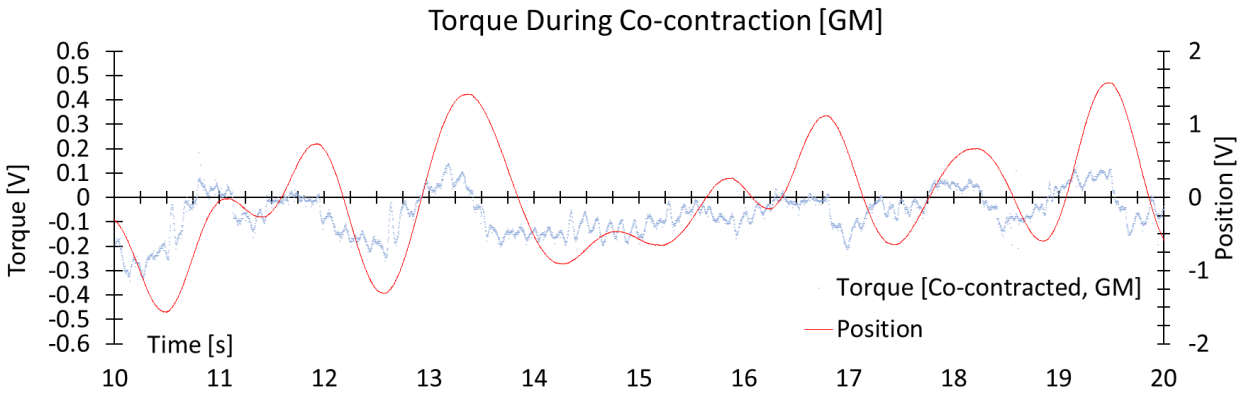

Figure 28: Torque values for the Random stimulus during co-contraction for GM.

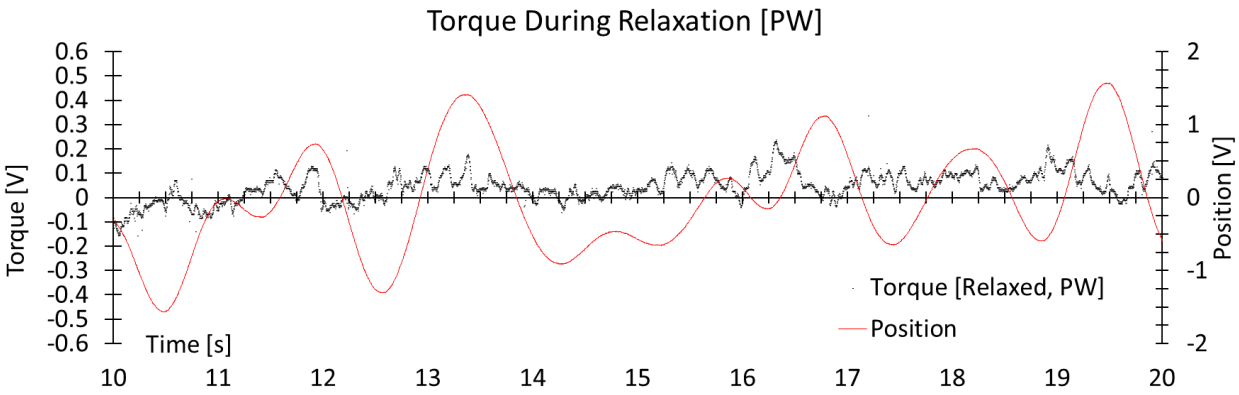

Figure 29: Torque values for the Random stimulus during relaxation for PW.

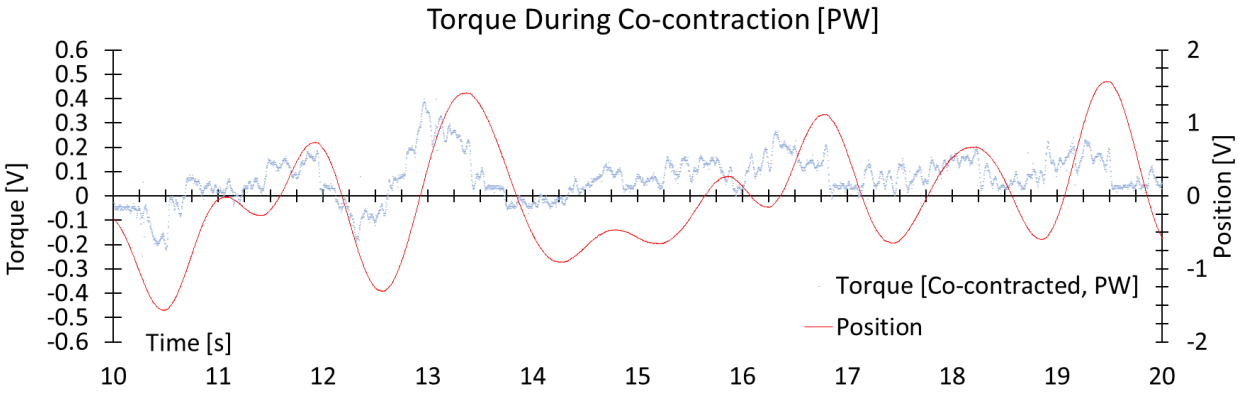

Figure 30: Torque values for the Random stimulus during co-contraction for PW.

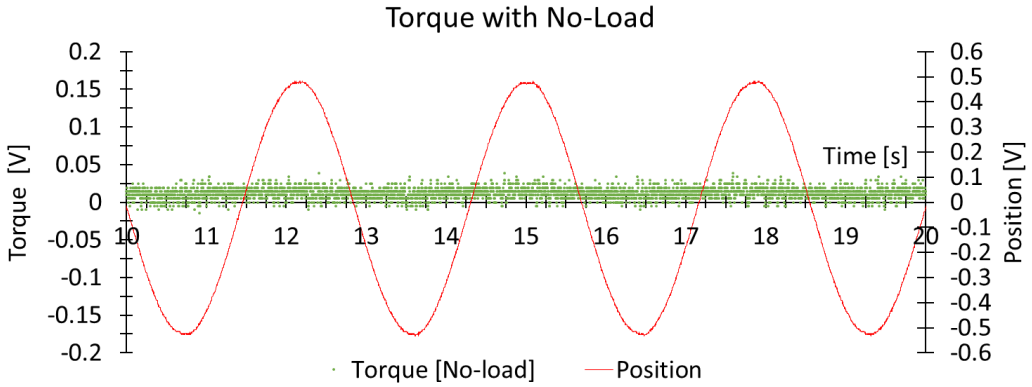

Figure 31: Torque values for the Sine stimulus with no load.

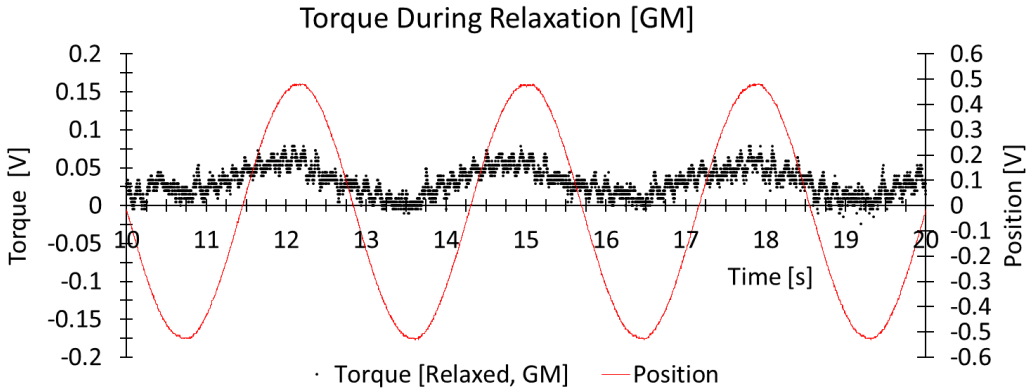

Figure 32: Torque values for the Sine stimulus during relaxation for GM.

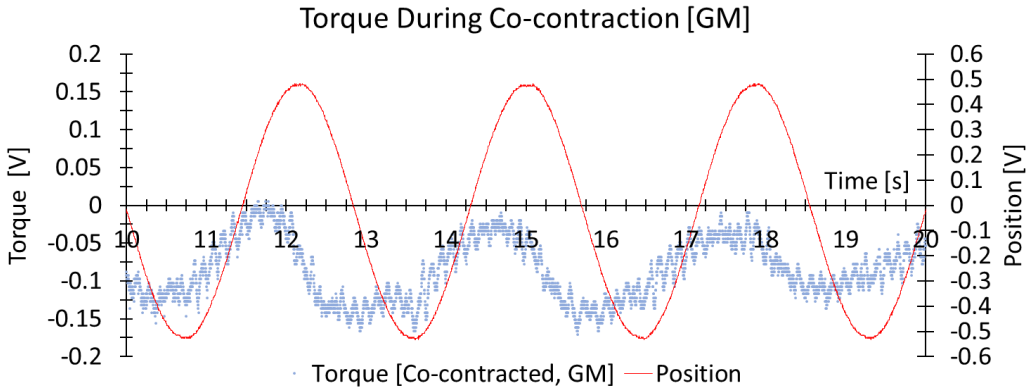

Figure 33: Torque values for the Sine stimulus during co-contraction for GM.

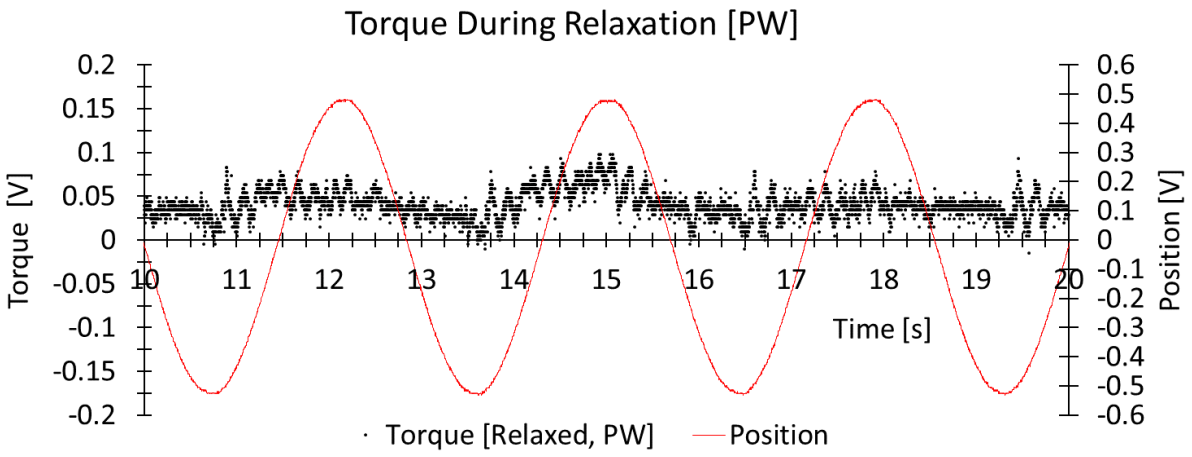

Figure 34: Torque values for the Sine stimulus during relaxation for PW.

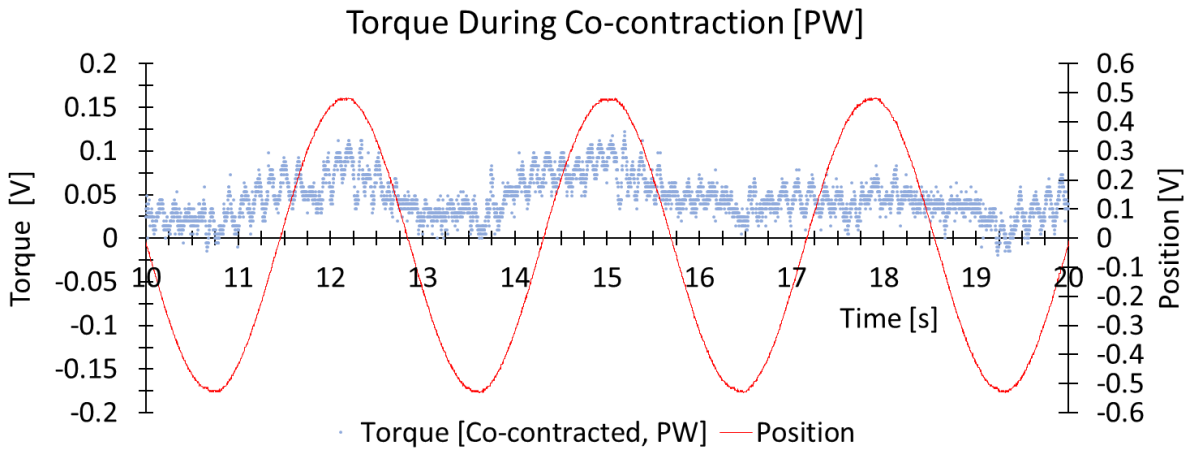

Figure 35: Torque values for the Sine stimulus during co-contraction for PW.

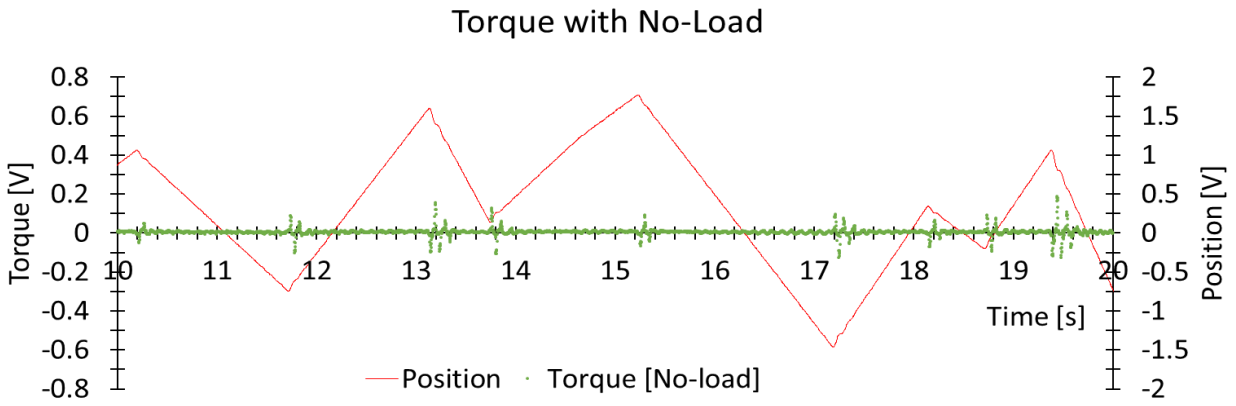

Figure 36: Torque values for the Ramp stimulus with no load.

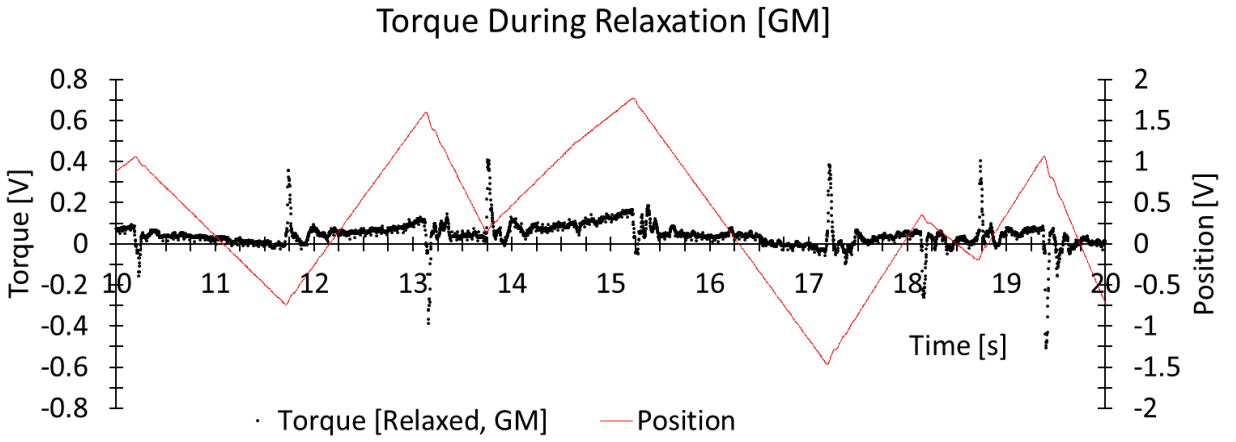

Figure 37: Torque values for the Ramp stimulus during relaxation for GM.

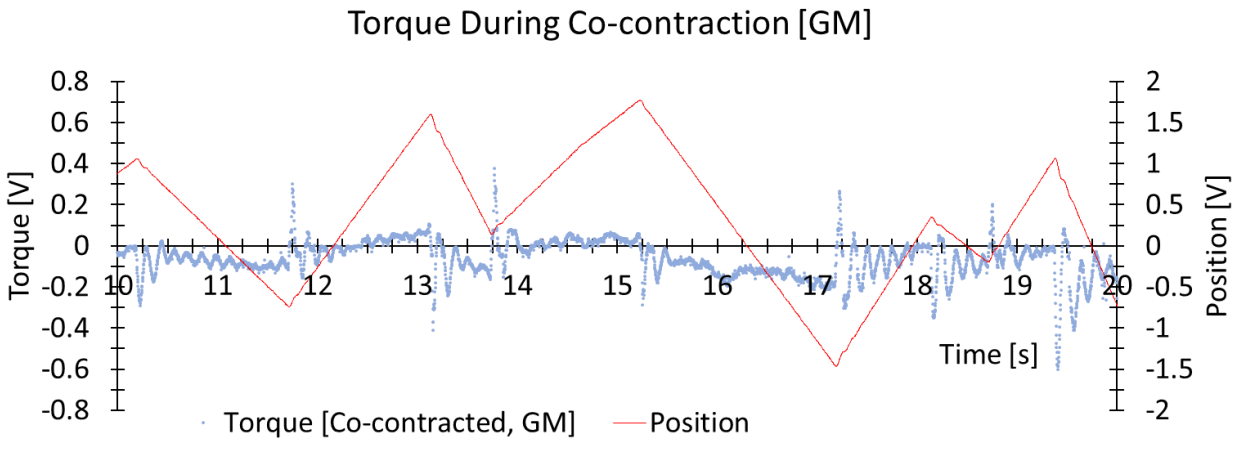

Figure 38: Torque values for the Ramp stimulus during co-contraction for GM.

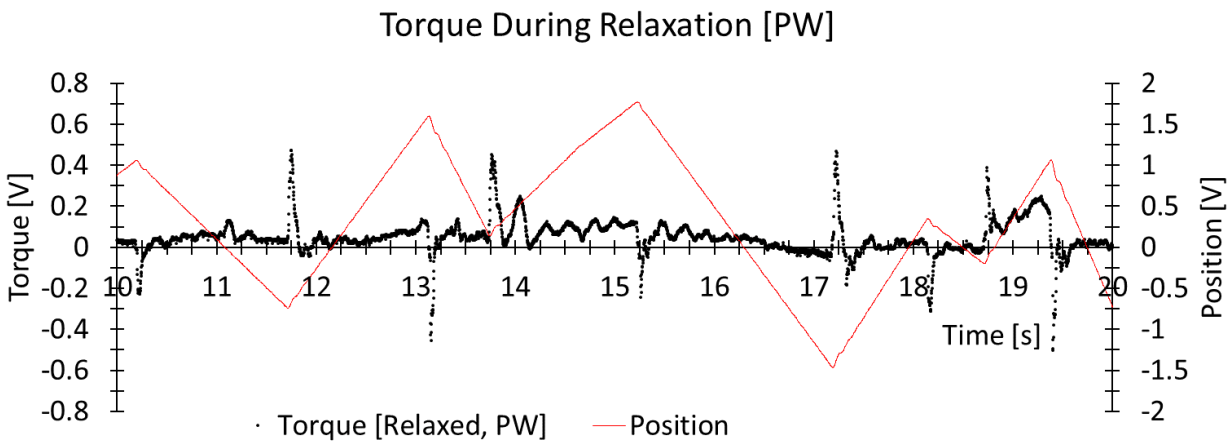

Figure 39: Torque values for the Ramp stimulus during relaxation for PW.

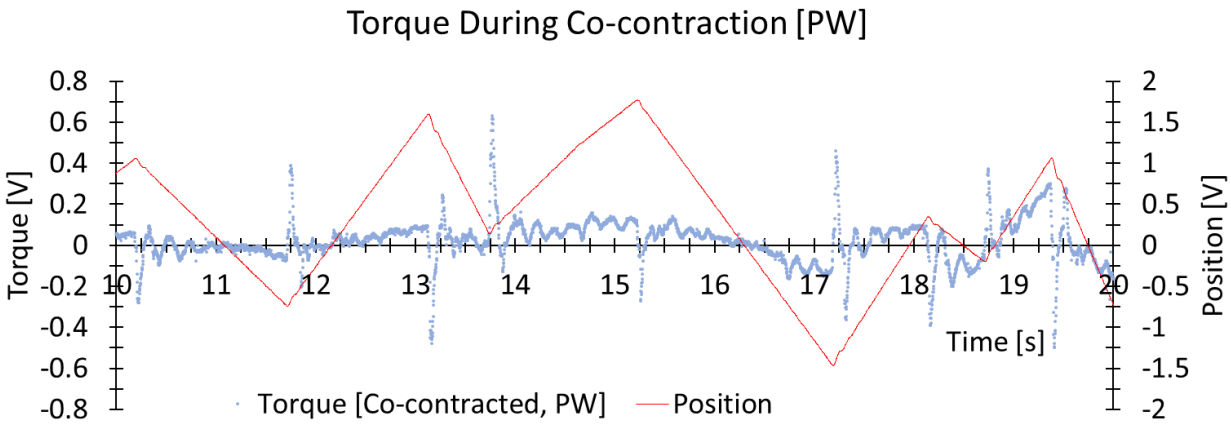

Figure 40: Torque values for the Ramp stimulus during co-contraction for PW.

Table 2: Mean and variance values for torque from the random stimulus

	Random Stimulus				
	No-load	GM (R)	GM (C)	PW (R)	PW (C)
Mean	0.01250	0.04254	-0.04380	0.04271	0.07009
Variance	0.00017	0.00277	0.01031	0.00337	0.00891

Note: (R) stands for relaxed arm, (C) stands for co-contracted arm. Mean and variance calculated for torque values which are measured in volts (V).

Table 3: Mean and variance values for torque from the ramp stimulus

	Ramp Stimulus				
	No-load	GM (R)	GM (C)	PW (R)	PW (C)
Mean	0.01205	0.03047	-0.04883	0.03382	0.01974
Variance	0.00209	0.00411	0.00920	0.00628	0.01189

Note: (R) stands for relaxed arm, (C) stands for co-contracted arm. Mean and variance calculated for torque values which are measured in volts (V).

Table 4: Mean and variance values for torque from the sine stimulus

	Sine Stimulus				
	No-load	GM (R)	GM (C)	PW (R)	PW (C)
Mean	0.01206	0.03145	-0.04351	0.04300	0.04835
Variance	0.00021	0.00038	0.00227	0.00037	0.00098

Note: (R) stands for relaxed arm, (C) stands for co-contracted arm. Mean and variance calculated for torque values which are measured in volts (V).

Stimulus Frequency Content

A Discrete Fourier Transform (DFT) was conducted, based on the chirp-z algorithm, on the sine and random position data to determine the frequency content of each waveform. The sine data had a peak magnitude at 0.35 Hz which is the known frequency content of the sine wave. The random signal had many peak magnitudes because it consisted of varying different sinusoidal signals. The frequency content of the waveform will never change with this setup because the motor controls the sling and does not allow for any position differences because of the negative feedback loop with the controller. This is shown in the graph below where the peak magnitudes for relaxed and co-contracted trials are the same.

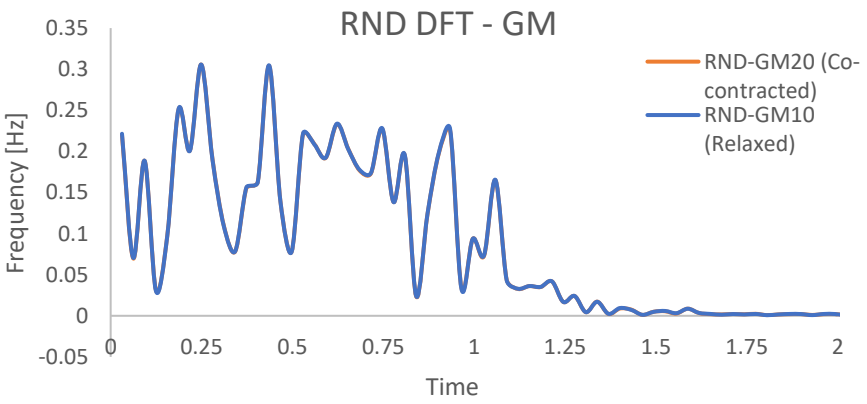

Figure 41: Frequency content of position in the random stimulus

Device Rumble

Roll, pitch and yaw were measured using a magnetic tracker and tracking device, which was attached directly behind the elbow on the rigid arm sling at the point of rotation. The roll and the pitch are of interest because there is a slight amount of play in the device due to space between the gear teeth in the transmission. The values of roll, seen in (Figure 46 and Figure 47), were less when there was no load in the device but there was no significant difference between the relaxed and co-contracted phases. The reverse was the case for pitch (Figure 44 and Figure 45), which was higher when there was no load than while tests were run. Like the roll values, the measured pitches during co-contraction and during

relaxation were remarkably similar. The measured yaw (Figure 42 and Figure 43) should have changed a lot because that was the orientation of movement but it seemed to change the least.

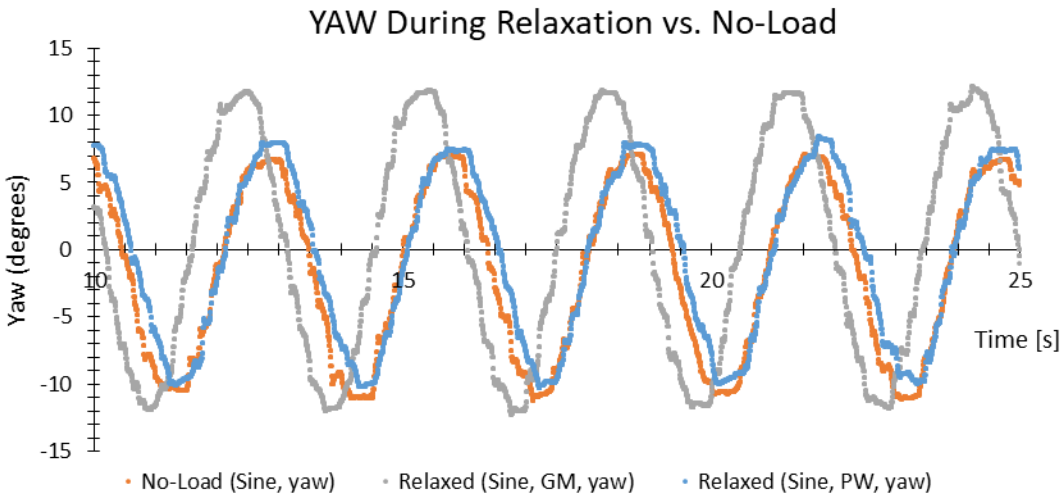

Figure 42: Yaw of the device during relaxation for GM and PW vs. during no-load condition.

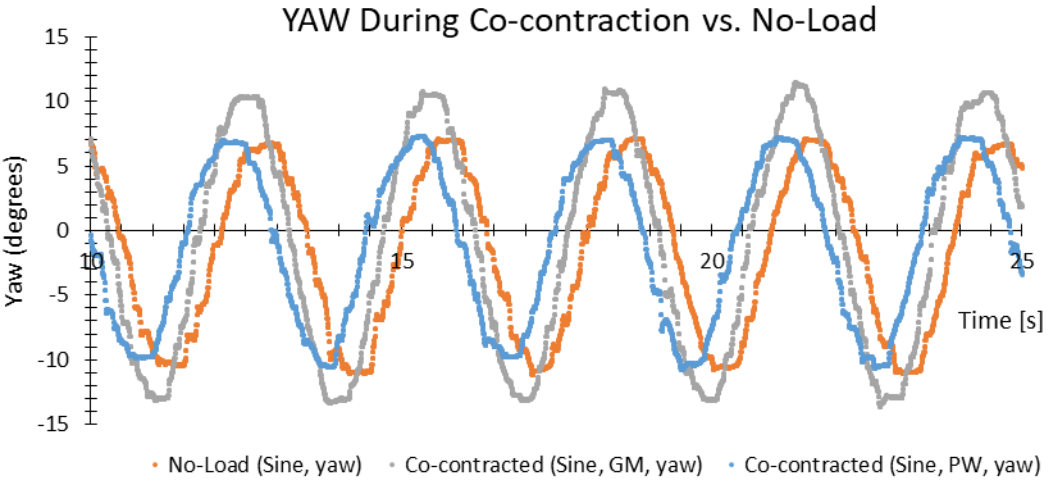

Figure 43: Yaw of the device during co-contraction for GM and PW vs. during no-load condition.

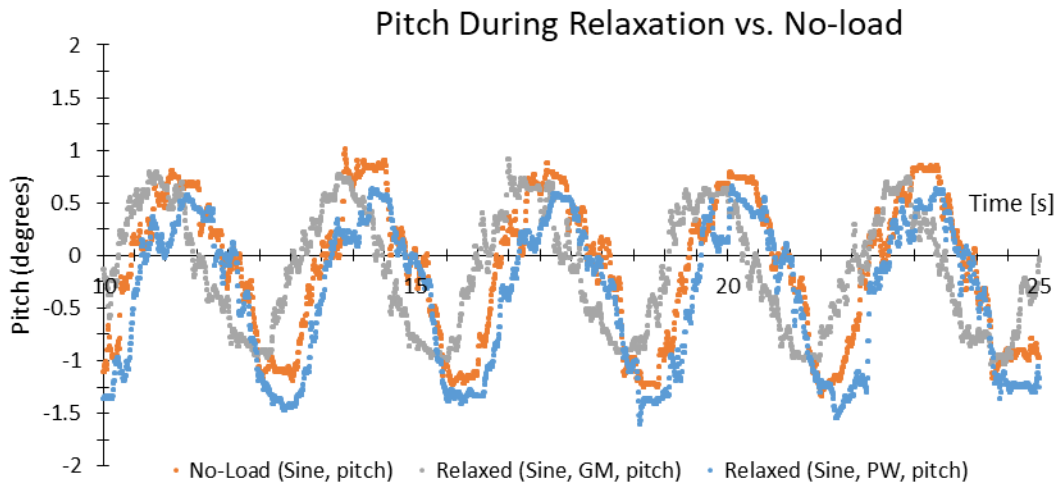

Figure 44: Pitch of the device during relaxation for GM and PW vs. during no-load condition.

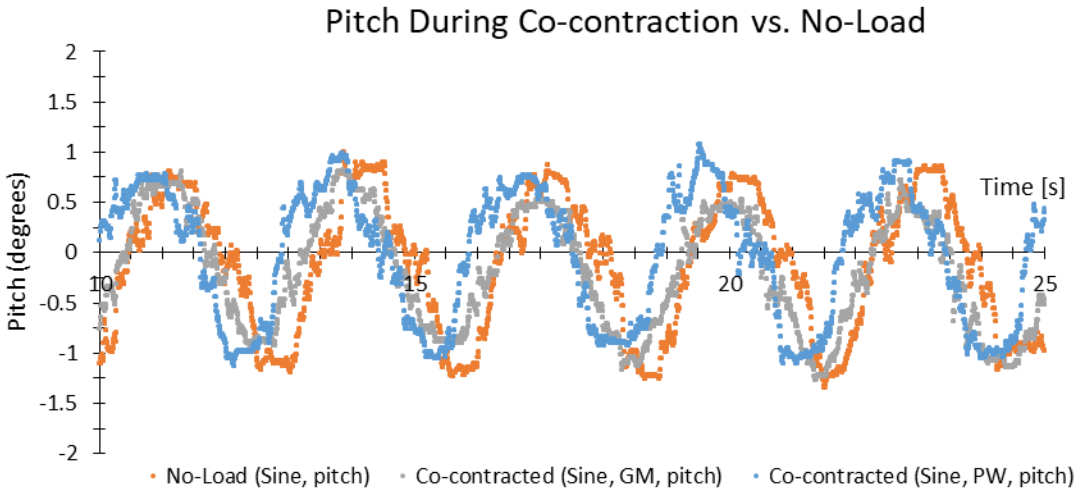

Figure 45: Pitch of the device during co-contraction for GM and PW vs. during no-load condition.

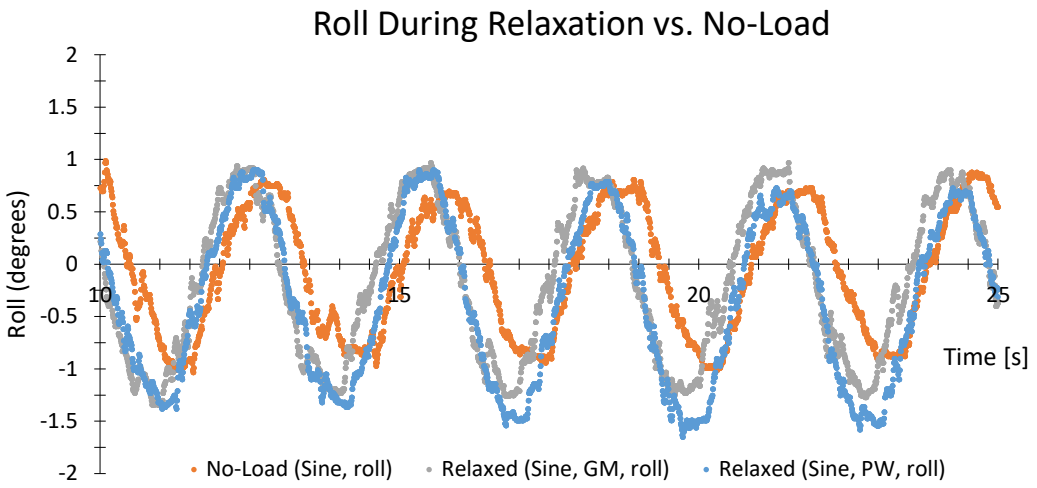

Figure 46: Roll of the device during relaxation for GM and PW vs. during no-load condition.

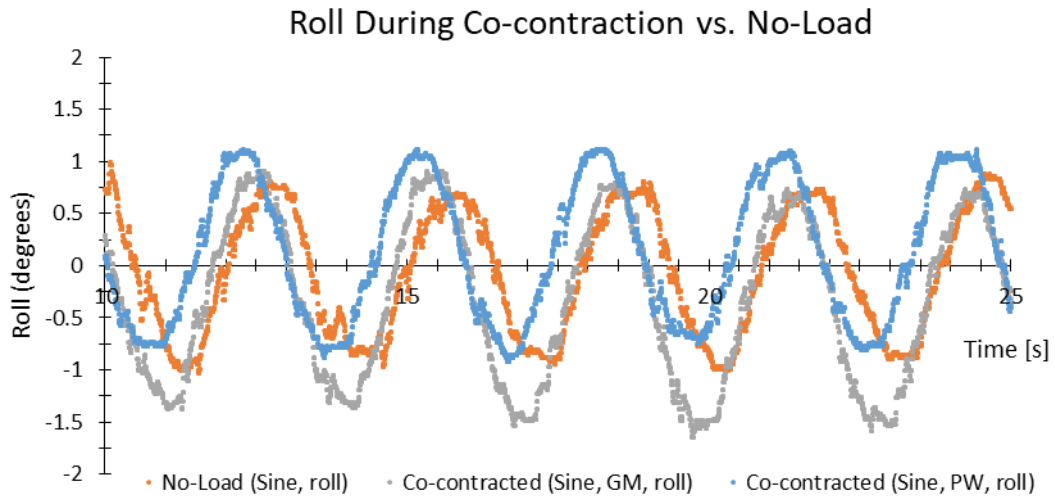

Figure 47: Roll of the device during co-contraction for GM and PW vs. during no-load condition.

V. Discussion

Sine, Discussion Ramp and Random Waveform Characterization

The main finding of the current study was the ability to objectively determine torque needed to flex and extend the elbow joint with respect to a specific stimulus signal. The random and sine signals show promise but there was too much force behind the abrupt changes of direction during the ramp stimulus and it does not mimic natural movement, nor does it mimic the clinical exam used to determine rigidity. These abrupt, sudden changes in direction, accentuated due to the negative feedback loop, led to similar torque values during relaxation and co-contraction and seemed to lightly shake the table while tests were being run. As such the ramp3.dat stimulus used in present form is not recommended, however a ramp and hold stimulus, which allows for softening of the abrupt changes, remains a possible solution.

During the relaxation tests of the random stimulus, most of the peaks in torque were accompanied by larger amplitude peaks during co-contraction. Although in (Figure 28), the torque signal during co-contraction appears to have an offset and two of the peak torque values during relaxation are larger than their co-contraction counterparts. The torque transducer, is directional, meaning that a value below zero indicates torque in the opposite direction, not a lack of torque. However, human error is likely as this offset was repeated by person 1 in the sine tests (Figure 33) but did not occur for person 2 in either test. Another possible reason could be attempted resistance to the movement by doing more than just co-contracting the muscles surrounding the elbow. In this case though the two peaks shown during the relaxation phase look larger than the co-contraction peaks prompting further explanation. Without measuring muscle activity during co-contraction and relaxation we cannot determine the exact reason for these peak magnitudes. However, they occur at the highest velocities of the stimulus and seem to be prompted by a change in direction. These larger magnitude peaks during relaxation could also be showing a natural reaction of the body to co-contract due to sudden change in direction and high speeds, like those in the ramp stimulus.

For the sine waves, the torque values appear to be larger during co-contraction than they are during relaxation although the offset was still present for person 1. Because we were unable to measure co-contraction in the surrounding muscles, we cannot definitively determine a cause for the offset or the torque peaks during the relaxation phase.

Calculated Variance

Mean and variance were both calculated for torque in each trial and for each person. The variances are all extremely small and instead of looking at the variance itself, the proportion of relaxed phase variance to co-contracted phase variance was calculated. Even though the variances overall are low, meaning the spread beyond the median is small, the variance for the co-contracted phase shows a value at least 25% higher than that of the relaxed phase in the sine and random stimuli. This would mean that average torque values are higher in the co-contraction phase than during the relaxed phase. During all three stimuli, and with each of the subjects the calculated variances were higher in the co-contracted data than in the relaxed data although the variances from the ramp data had the lowest increases.

Frequency Response (DFT)

The DFT of a stimulus during relaxation and co-contraction will look the same regardless of torque because the position of the signal is the same for each change. DFT measures frequency content of a waveform and because of the presence of the negative feedback loop in the controller, the position data is the same during relaxation and co-contraction. The DFT of the random file has many different magnitude peaks relating to the changing frequency of the random stimulus. The sine stimulus used has only one peak at 0.35 Hz which is to be expected due to the known frequency content of the sine wave.

Limitations and Suggested Improvements

There were many limitations in this preliminary study, including the small sample size and the absence of PD patients. The device was also not evaluated for use in the vertical plane. Although the

results are repeatable, co-contraction was not constant throughout each test run or between stimuli and without further evaluation we would not be able to determine the varying degrees of co-contraction throughout the test. Each stimulus file was run multiple times before recorded tests were run and greater torque during co-contraction was a result in those as well. Though co-contraction is a good alternative in this situation, a preliminary study consisting of PD patients to see a comparison of torque in a PD patient population versus a control group should be completed.

In addition to the limitations of the study itself, there are a few serious factors with respect to clinical use that must be considered, including the backlash in the transmission which could be remediated by removing the transmission altogether as the servo motor was made for precise movement. Unfortunately, the transmission is what allows the shaft-sling assembly to rotate into the lower position and the device would no longer have the capability of measuring in two different planes. In order to retain this ability, transmission updates to decrease the clearance between the gear teeth if possible or obtaining a higher precision transmission would decrease backlash.

The feedback mechanism also must be considered when selecting patients for a future study. Because the motor will force the patients arm to move regardless of ability, a patient's range must be examined before determining candidacy. While limits may be set to ensure the device does not exceed a certain angle of rotation, each participant should be evaluated for range of motion in their elbow joint prior to involvement to ensure safety.

The device is also not easily portable. It can be carried by a single person, one assembly at a time but it is bulky and unfortunately many of the components are heavy. There is also currently no height adjustment and so the device itself is not customizable to people of varying heights, or for those who cannot stand. The device is tall and therefore would need to be placed on a shorter table or an adjustable height stand so that it could easily be moved higher or lower to allow for height adjustments. On a standard height table, the device must be used while standing. Furthermore, there is no way to immobilize the rest of the patient's body during testing. A seated approach would allow for a smaller overall height range and test subjects could be restrained more easily.

While this is not a necessary upgrade, a modified arm sling would provide patients with more comfort, better restraint of the limb, and it would ensure that each patient's arm is tested about the same point. The current sling is made to be one size fits all with Velcro straps used to position the forearm and hold it in place, but it is not very comfortable. I suggest a modified partially 3D printed arm sling with the ability to increase length of the sling, and a manipulandum to ensure proper rotation of the wrist, similar to the example from Sin et al. (2019) These modifications would increase repeatability and provide comfort for the patient

Future Directions and Conclusions

Although this device has not yet been tested on PD patients, the preliminary results of torque measured in phases of co-contraction and relaxation during passive flexion and extension of the forearm of two healthy individuals proves that this device does effectively measure torque. In addition, the safety features included in the TTL safety circuit will allow for reliable operation of the device in a research setting. In correlation with the clinical standard subjective rating scales, this device could be used to objectively quantify torque, and therefore rigidity, in the elbow joint of patients to better understand the mechanisms of rigidity in those suffering from Parkinson's and other movement disorders.

References

1. Armstrong, M. J., & Okun, M. S. (2020). Diagnosis and Treatment of Parkinson Disease: A Review. *JAMA, 323*(6), 548–560. https://doi.org/10.1001/jama.2019.22360
2. Association, E. P. D. (2016). Rigidity. Retrieved from https://www.epda.eu.com/about-parkinsons/symptoms/motor-symptoms/rigidity/
3. Barmore, R. (n.d.). Stages of Parkinsons. Retrieved from https://www.parkinson.org/Understanding-Parkinsons/What-is-Parkinsons/Stages-of-Parkinsons
4. Bhidayasiri, R., & Martinez-Martin, P. (2017). Clinical Assessments in Parkinson's Disease: Scales and Monitoring. *Parkinson's Disease, 132,* 129-182.
5. Brookshire, B. (2019, December 6). Explainer: What is dopamine? Retrieved from https://www.sciencenewsforstudents.org/article/explainer-what-dopamine
6. Cano-de-la-Cuerda, R., Vela-Desojo, L., Miangolarra-Page, J., Macías-Macías, C., & Muñoz-Hellín, Y. (2011). Axial rigidity and quality of life in patients with Parkinson's disease: A preliminary study. Quality of Life Research, 20(6), 817-823.
7. Chunbao Wang, A., Lihong Duan, Qing Shi, Nibori, Miura, Sugamiya, . . . Weiguang Li. (2014). Development of a human-like motor nerve model to simulate the diseases effects on muscle tension for neurologic examination training. *2014 IEEE International Conference on Robotics and Biomimetics (ROBIO 2014),* 713-718.
8. Di Biase, Summa, Tosi, Taffoni, Marano, Cascio Rizzo, . . . Tombini. (2018). Quantitative Analysis of Bradykinesia and Rigidity in Parkinson's Disease. *Frontiers in Neurology, 9,* 121.
9. Downward, E. (2017). Diagnosing Parkinson's Disease: Rating Scales. Retrieved from https://parkinsonsdisease.net/diagnosis/rating-scales-staging/
10. Elkouzi, A. (n.d.). What Is Parkinson's? Retrieved from https://www.parkinson.org/understanding-parkinsons/what-is-parkinsons
11. Endo, T., Okuno, R., Yokoe, M., Akazawa, K., & Sakoda, S. (2009). A novel method for systematic analysis of rigidity in Parkinson's disease. Movement Disorders, 24(15), 2218-2224.
12. Goetz, C., Fahn, S., Martinez-Martin, P., Poewe, W., Sampaio, C., Stebbins, G., . . . LaPelle, N. (2007). Movement Disorder Society-sponsored revision of the Unified Parkinson's Disease Rating Scale (MDS-UPDRS): Process, format, and clinimetric testing plan. Movement Disorders, 22(1), 41-47.
13. Goetz, C., Luo, S., Wang, L., Tilley, B., Lapelle, N., & Stebbins, G. (2015). Handling missing values in the MDS-UPDRS. *Movement Disorders, 30*(12), 1632-1638.
14. Goetz, C., Poewe, W., Rascol, O., Sampaio, C., Stebbins, G., Counsell, C., . . . Seidl, L. (2004). Movement Disorder Society Task Force report on the Hoehn and Yahr staging scale: Status and recommendations The Movement Disorder Society Task Force on rating scales for Parkinson's disease. *Movement Disorders, 19*(9), 1020-1028.
15. Goetz, C., Poewe, W., Rascol, O., Sampaio, C., Stebbins, G., Counsell, C., . . . Seidl, L. (2004). Movement Disorder Society Task Force report on the Hoehn and Yahr staging scale: Status and recommendations The Movement Disorder Society Task Force on rating scales for Parkinson's disease. *Movement Disorders, 19*(9), 1020-1028.
16. Goetz, C., Tilley, B., Shaftman, S., Stebbins, G., Fahn, S., Martinez-Martin, P., . . . LaPelle, N. (2008). Movement Disorder Society-sponsored revision of the Unified Parkinson's Disease Rating Scale (MDS-UPDRS): Scale presentation and clinimetric testing results. *Movement Disorders, 23*(15), 2129-2170.
17. Guttman, M., Kish, S., & Furukawa, Y. (2003). Current concepts in the diagnosis and management of Parkinson's disease. Canadian Medical Association Journal, 168(3), 293-301.
18. Health Related Quality of Life and Well-Being. (2010). Retrieved from https://www.healthypeople.gov/2020/about/foundation-health-measures/Health-Related-Quality-of-Life-and-Well-Being

19. Holden, S., Finseth, T., Sillau, S., & Berman, B. (2018). Progression of MDS-UPDRS Scores Over Five Years in De Novo Parkinson Disease from the Parkinson's Progression Markers Initiative Cohort. *Movement Disorders Clinical Practice, 5*(1), 47-53.
20. Hong, M., Perlmutter, J., & Earhart, G. (2007). Enhancement of rigidity in Parkinson's disease with activation. *Movement Disorders, 22*(8), 1164-1168.
21. Huang, H., Ju, M., & Lin, C. (2016). Flexor and extensor muscle tone evaluated using the quantitative pendulum test in stroke and parkinsonian patients. *Journal of Clinical Neuroscience, 27*, 48-52.
22. Kirollos, C., Charlett, A., O' Neill, C. J. A., Kosik, R., Mozol, K., Purkiss, A. G., . . . Dobbs, R. J. (1996). Objective measurement of activation of rigidity: Diagnostic, pathogenetic and therapeutic implications in parkinsonism. *British Journal of Clinical Pharmacology, 41*(6), 557-564.
23. Lee, H., Huang, Y., Chen, J., & Hwang, I. (2002). Quantitative analysis of the velocity related pathophysiology of spasticity and rigidity in the elbow flexors. *Journal of Neurology, Neurosurgery & Psychiatry, 72*(5), 621-629.
24. Little, S., Joundi, R., Tan, A., Pogosyan, H., Forrow, A., Joint, B., . . . Brown, L. (2012). A torque-based method demonstrates increased rigidity in Parkinson's disease during low-frequency stimulation. *Experimental Brain Research, 219*(4), 499-506.
25. Mantri, S., & Morley, J. (2018, May). Prodromal and Early Parkinson's Disease Diagnosis. Retrieved from https://practicalneurology.com/articles/2018-may/prodromal-and-early-parkinsons-disease-diagnosis
26. María Del Rosario Ferreira-Sánchez, Marcos Moreno-Verdú, & Roberto Cano-de-La-Cuerda. (2020). Quantitative Measurement of Rigidity in Parkinson's Disease: A Systematic Review. *Sensors, 20*(3), 880.
27. Martinez-Martin, P., Rodriguez-Blazquez, C., Forjaz, M., Alvarez-Sanchez, M., Arakaki, T., Bergareche-Yarza, A., . . . Goetz, C. (2014). Relationship between the MDS-UPDRS domains and the health-related quality of life of Parkinson's disease patients. *European Journal of Neurology, 21*(3), 519-524.
28. Martinez-Martin, P., Skorvanek, M., Rojo-Abuin, J., Gregova, Z., Stebbins, G., & Goetz, C. (2018). Validation study of the hoehn and yahr scale included in the MDS-UPDRS. *Movement Disorders, 33*(4), 651-652.
29. Merello, M., & Antonini, A. (2019). Parkinson's Disease and Parkinsonism. Retrieved from https://www.movementdisorders.org/MDS/About/Movement-Disorder-Overviews/Parkinsons-Disease--Parkinsonism.htm#
30. Parkinson's Disease vs. Parkinsonism. (n.d.). Retrieved from https://www.parkinson.org/pd-library/fact-sheets/parkinsonism-vs-parkinsons-disease
31. Perera, T., Lee, W., Jones, M., Tan, J., Proud, E., Begg, A., . . . Mcdermott, H. (2019). A palm-worn device to quantify rigidity in Parkinson's disease. Journal of Neuroscience Methods, 317, 113-120.
32. Perry, S. (2015, October 22). Dopamine and Movement. Retrieved from https://www.brainfacts.org/thinking-sensing-and-behaving/movement/2015/dopamine-and-movement
33. Postuma, R., & Berg, D. (2016). MDS Clinical Diagnostic Criteria for Parkinson's Disease. *Neurology, 86*(S16), Neurology, 2016 Apr 5, Vol.86 Suppl 16.
34. Postuma, R., Poewe, W., Litvan, I., Lewis, S., Lang, A., Halliday, G., . . . Berg, D. (2018). Validation of the MDS clinical diagnostic criteria for Parkinson's disease. *Movement Disorders, 33*(10), 1601-1608.
35. Powell, D., Joseph Threlkeld, A., Fang, X., Muthumani, A., & Xia, R. (2012). Amplitude- and velocity-dependency of rigidity measured at the wrist in Parkinson's disease. *Clinical Neurophysiology, 123*(4), 764-773.
36. Prochazka, A., Bennett, D., Stephens, M., Patrick, S., Sears-Duru, R., Roberts, T., & Jhamandas, J. (1997). Measurement of rigidity in Parkinson's disease. *Movement Disorders, 12*(1), 24-32.
37. Relja, M. A., Petravic, D., & Kolaj, M. (1996). Quantifying Rigidity with a New Computerized Elbow Device. *Clinical Neuropharmacology, 19*(2), 148-156.

38. Rovini, E., Maremmani, C., & Cavallo, F. (2017). How Wearable Sensors Can Support Parkinson's Disease Diagnosis and Treatment: A Systematic Review. *Frontiers In Neuroscience, 11*, 555.
39. Scharre, D., & Mahler, M. (1994). PARKINSONS-DISEASE - MAKING THE DIAGNOSIS, SELECTING DRUG THERAPIES. *Geriatrics, 49*(10), 14.
40. Sepehri, B., Esteki, A., Ebrahimi-Takamjani, E., Shahidi, G., Khamseh, F., & Moinodin, M. (2007). Quantification of Rigidity in Parkinson's Disease. Annals of Biomedical Engineering, 35(12), 2196-2203.
41. Sin, M., Kim, W.-S., & Cho, K., Paik, N.-J. (2019, June 12). Isokinetic Robotic Device to Improve Test-Retest and Inter-Rater Reliability for Stretch Reflex Measurements in Stroke Patients with Spasticity: Protocol. Retrieved from https://www.jove.com/video/59814/isokinetic-robotic-device-to-improve-test-retest-inter-rater
42. Spears, C. (n.d.) a. Non-Movement Symptoms. Retrieved from https://www.parkinson.org/Understanding-Parkinsons/Non-Movement-Symptoms
43. Spears, C. (n.d.) b. Movement Symptoms. Retrieved from https://www.parkinson.org/Understanding-Parkinsons/Movement-Symptoms
44. Triarhou, L. C. (2000-2013). Dopamine and Parkinson's Disease. Retrieved from https://www.ncbi.nlm.nih.gov/books/NBK6271/
45. Tysnes, O., & Storstein, A. (2017). Epidemiology of Parkinson's disease. *Journal of Neural Transmission, 124*(8), 901-905.
46. Xia, R., Powell, D., Rymer, W., Hanson, Z., Fang, N., & Threlkeld, X. (2011). Differentiation between the contributions of shortening reaction and stretch-induced inhibition to rigidity in Parkinson's disease. *Experimental Brain Research, 209*(4), 609-618.

Appendix 1: Parts List

Part Name	Part Number	Qty.	Manufacturer
12 VDC Power Supply	SDI18-12-UC-P5	1	CUI Inc.
20 KΩ Multi-turn Precision Potentiometer	3540S-1-203L	1	Bourns
12000µF Powerlytic™ Capacitor	36DY	1	Vishay Sprague Powerlytic™
Medical Grade Isolation Transformer	ISB-060A	1	Toroid
Photologic Slotted Optical Switch	OPB991	2	TT Electronics
Servo Amplifier/Controller	25A20	1	Advanced Motion Controls
Servo Motor	JR16M4CH/ENC	1	Kollmorgen
Torque Transducer	QSFK-9/J301-01	1	Sensotec
Transducer Power Supply	Model PSM-R	1	Transducer Techniques
Transmission	Unknown	1	Motovario
Variac Transformer	1010B	1	Staco
100K Ω Trimpot®	W104	1	Bourns
10K Ω Trimpot®	W103	1	Bourns
1K Ω Trimpot®	W102	2	Bourns
20K Ω Trimpot®	W203	1	Bourns
3-Lead Bi-Color LED	PM53-KNBCW12.0	1	Bivar
500 Ω Trimpot®	W501	1	Bourns
5K Ω Trimpot®	W502	1	Bourns
5V Fixed Voltage Regulator	LM340T	1	Texas Instruments
Adjustable Linear Voltage Regulator	LM317T	1	STMicroelectronics
Capacitors	-----	12	See Appendix 2
Diodes	1N914	3	Vishay
Dual 5-Input Positive-NOR Gate	SN74F260	1	Texas Instruments
Heat Sink	-----	2	N/A
Hex Inverter	SN74LS04N	1	Texas Instruments
Monolithic Sample-and-Hold Circuit	LF398N	1	Texas Instruments
Push-Button Switch	30-6	2	Grayhill
Quad Differential Comparator	LM339	1	Texas Instruments
Quadruple S-R Latch	SN74LS279A	1	Texas Instruments
Resistors	-----	30	See Appendix 2
Re-triggerable Monostable Multivibrator "One-shot"	SN74LS123N	1	Texas Instruments
Silicon NPN Transistor	2N2222	1	Central Semiconductor Corp.
Switched-Capacitor Voltage Converters with Regulators	LT1054	1	Texas Instruments
Ultraprecision Operational Amplifier	OP177	3	Analog Devices, Inc.

Appendix 2: Resistor and Capacitor List

Resistors	
Number:	**Value:**
R1	4.02K Ω
R2	5.11K Ω
R3	5.11K Ω
R4	301 Ω
R5	126 Ω
R6	309 Ω
R7	105 Ω
R8	126 Ω
R9	309 Ω
R10	105 Ω
R11	301 Ω
R12	301 Ω
R13	30.1 Ω
R14	20K Ω
R15	180K Ω
R16	5.11K Ω
R17	10K Ω
R18	475 Ω
R19	5.49K Ω
R20	174 Ω
R21	15K Ω
R22	15K Ω
R23	15K Ω
R24	13.7K Ω
R25	13.3K Ω
R26	1K Ω
R27	4.99K Ω
R28	5.23K Ω
R29	5.23K Ω
R30	5.23K Ω

Capacitors		
Number:	**Value:**	**Type:**
C1	10 µF	tantalum
C2	22 µF	tantalum
C3	0.0022 µF	mylar
C4	100 µF	electrolytic
C5	0.1 µF	mylar
C6	2.2 µF	mylar
C7	2.2 µF	mylar
C8	100 µF	electrolytic
C9	0.1 µF	mylar
C10	1 µF	tantalum
C11	10 µF	electrolytic
C12	0.1 µF	mylar